

1 **Proteomics and phosphoproteomics profiling in glutamatergic neurons and microglia in**  
2 **an iPSC model of Jansen de Vries Syndrome**

3 Jennifer T. Aguilan<sup>1\*</sup>, Erika Pedrosa<sup>2\*</sup>, Hedwig Dolstra<sup>2</sup>, Refia Nur Baykara<sup>2</sup>, Jesse Barnes<sup>2</sup>,  
4 Jinghang Zhang<sup>3</sup>, Simone Sidoli<sup>4</sup>, Herbert M. Lachman<sup>2,5,6,7#</sup>

5 #corresponding author

6 \*Contributed equally

7

8 <sup>1</sup> Jennifer Aguilan

9 Department of Pathology

10 Albert Einstein College of Medicine

11 1300 Morris Park Ave. Bronx, NY, 10461

12 [jennifer.aguilan@einsteinmed.edu](mailto:jennifer.aguilan@einsteinmed.edu)

13

14 <sup>2</sup> Erika Pedrosa

15 Department of Psychiatry and Behavioral Sciences

16 Albert Einstein College of Medicine

17 1300 Morris Park Ave. Bronx, NY, 10461

18 [erika.pedrosa@einsteinmed.edu](mailto:erika.pedrosa@einsteinmed.edu)

19

20 <sup>2</sup> Hedwig Dolstra

21 Department of Psychiatry and Behavioral Sciences

22 Albert Einstein College of Medicine

23 1300 Morris Park Ave. Bronx, NY, 10461

24 [hedwigdolstra@gmail.com](mailto:hedwigdolstra@gmail.com)

25

26 <sup>2</sup> Refia Nur Baykara

27 Department of Psychiatry and Behavioral Science

28 Albert Einstein College of Medicine

29 1300 Morris Park Ave. Bronx, NY, 10461

30 [refianurbaykara95@gmail.com](mailto:refianurbaykara95@gmail.com)

31

32 <sup>2</sup> Jesse Barnes

33 Department of Psychiatry and Behavioral Sciences

34 Albert Einstein College of Medicine

35 1300 Morris Park Ave. Bronx, NY, 10461

36 [barnesjesse11@gmail.com](mailto:barnesjesse11@gmail.com)

37

38 <sup>3</sup> Jinghang Zhan

39 Department of Microbiology & Immunology

40 Albert Einstein College of Medicine

41 1300 Morris Park Ave. Bronx, NY, 10461

42 [jinghang.zhang@einsteinmed.edu](mailto:jinghang.zhang@einsteinmed.edu)

43

44 <sup>4</sup> Simone Sidoli

45 Department of Biochemistry

46 Albert Einstein College of Medicine

47 1300 Morris Park Ave. Bronx, NY, 10461

48 [simone.sidoli@gmail.com](mailto:simone.sidoli@gmail.com)

49

50 <sup>2,5,6,7</sup> Herbert M. Lachman

51 Department of Psychiatry and Behavioral Sciences

52 Department of Medicine

53 Dominick P. Purpura Department of Neuroscience

54 Department of Genetics

55 Albert Einstein College of Medicine

56 1300 Morris Park Ave. Bronx, NY, 10461

57 Herb.Lachman@einsteinmed.edu

58

59 Key words: pediatric acute-onset neuropsychiatric syndrome (PANS), autism, regression,

60 POGZ, ubiquitin ligase, UBR4, SRRM1, NUCKS1, PPM1D, Jansen de Vries Syndrome

61

62

63

64 **Abstract**

65 **Background:** Jansen de Vries Syndrome (JdVS) is a rare neurodevelopmental disorder (NDD)  
66 caused by gain-of-function (GOF) truncating mutations in *PPM1D* exons 5 or 6. *PPM1D* is a  
67 serine/threonine phosphatase that plays an important role in the DNA damage response (DDR)  
68 by negatively regulating TP53 (P53). JdVS-associated mutations lead to the formation of a  
69 truncated *PPM1D* protein that retains catalytic activity and has a GOF effect because of  
70 reduced degradation. Somatic *PPM1D* exons 5 and 6 truncating mutations are well-established  
71 factors in a number of cancers, due to excessive dephosphorylation and reduced function of  
72 P53 and other substrates involved in DDR. Children with JdVS have a variety of  
73 neurodevelopmental, psychiatric, and physical problems. In addition, a small fraction has acute  
74 neuropsychiatric decompensation apparently triggered by infection or severe non-infectious  
75 environmental stress factors.

76 **Methods:** To understand the molecular basis of JdVS, we developed an induced pluripotent  
77 stem cell (iPSC) model system. iPSCs heterozygous for the truncating variant (*PPM1D*<sup>+tr</sup>), were  
78 made from a patient, and control lines engineered using CRISPR-Cas9 gene editing.  
79 Proteomics and phosphoproteomics analyses were carried out on iPSC-derived glutamatergic  
80 neurons and microglia from three control and three *PPM1D*<sup>+tr</sup> iPSC lines. We also analyzed the  
81 effect of the TLR4 agonist, lipopolysaccharide, to understand how activation of the innate  
82 immune system in microglia could account for acute behavioral decompensation.

83 **Results:** One of the major findings was the downregulation of POGZ in unstimulated microglia.  
84 Since loss-of-function variants in the *POGZ* gene are well-known causes of autism spectrum  
85 disorder, the decrease in *PPM1D*<sup>+tr</sup> microglia suggests this plays a role in the  
86 neurodevelopmental aspects of JdVS. In addition, neurons, baseline, and LPS-stimulated  
87 microglia show marked alterations in the expression of several E3 ubiquitin ligases, most  
88 notably UBR4, and regulators of innate immunity, chromatin structure, ErbB signaling, and  
89 splicing. In addition, pathway analysis points to overlap with neurodegenerative disorders.

90 **Limitations:** Owing to the cost and labor-intensive nature of iPSC research, the sample size  
91 was small.

92 **Conclusions:** Our findings provide insight into the molecular basis of JdVS and can be  
93 extrapolated to understand neuropsychiatric decompensation that occurs in subgroups of  
94 patients with ASD and other NDDs.

95

96

## 97 **Introduction**

98 Jansen de Vries Syndrome (JdVS) (OMIM 617450) is a recently discovered  
99 neurodevelopmental disorder (NDD) caused by truncating mutations in *PPM1D* exons 5 or 6 (1-  
100 4). It is characterized by mild to severe intellectual disability, anxiety disorder, attention deficit  
101 hyperactivity disorder (ADHD), obsessive behavior, hypotonia, sensory integration problems,  
102 and in some cases, autism spectrum disorder (ASD). In addition, feeding difficulties and  
103 gastrointestinal problems (e.g., constipation, esophageal reflux, and cyclic vomiting syndrome)  
104 are common. Approximately half of the reported cases have an increase in childhood infections,  
105 although this has not been systematically evaluated and the pathogenesis has not been  
106 established. *PPM1D* codes for a member of the PP2C serine/threonine phosphatase family. So  
107 far, every *PPM1D* mutation found in JdVS is predicted to translate into a truncated protein (e.g.,  
108 nonsense mutations and frameshifts) because of the loss of C-terminal amino acids. The  
109 catalytic domain encoded largely by exons 1-4 is preserved, and an increase in *PPM1D* half-life  
110 occurs because truncated proteins lose a degradation signal that maps within the terminal 65  
111 amino acids (5,6).

112  
113 *PPM1D* is a well-known tumor suppressor gene, acting as a negative regulator of P53 and other  
114 proteins involved in the DNA damage response (DDR) pathway, such as MDM2, ATM, CHK1,  
115 CHK2, ATR, and H2AX (7-9). Somatic GOF truncating mutations in exons 5 or 6 have been  
116 found in a variety of cancers (7-14). Cancer risk in JdVS has not yet been established, although  
117 a normal P53 response to ionizing radiation was found in EB-transformed lymphocytes derived  
118 from children with JdVS (4).

119  
120 In addition to the neurodevelopmental and psychiatric features of JdVS, a small subgroup of  
121 patients experience behavioral decompensation that appears to be linked to infection or severe  
122 physical stress. One patient we identified was diagnosed with pediatric acute-onset

123 neuropsychiatric syndrome (PANS) as a child, several years prior to exome sequencing for  
124 NDD revealed a typical *PPM1D* truncating variant (15). PANS is an enigmatic,  
125 neuroinflammatory disorder characterized by the abrupt onset of severe neurological and  
126 psychiatric symptoms that includes obsessive-compulsive disorder (OCD), restricted eating,  
127 anxiety, cognitive deficits with academic regression, disrupted sleep, rage, mood disturbance,  
128 joint inflammation, and autonomic nervous system disturbances (e.g., enuresis, postural  
129 orthostatic tachycardia syndrome) (16-18). Subsequently, we identified two other JdVS case in  
130 which severe behavioral and motor regression occurred following infection and noninfectious  
131 triggers.

132  
133 Mouse *Ppm1d* knockout (KO) models have been developed, which show effects on dendritic  
134 spine morphology and memory processes, a disturbance in T- and B-lymphocyte differentiation,  
135 proliferation, cytokine production, and an increase in phagocytosis and autophagy in peripheral  
136 macrophages (19-22). However, a mouse *Ppm1d* KO is not an appropriate model for JdVS  
137 GOF variants. Consequently, in order to understand the underlying molecular basis of truncated  
138 PPM1D on neuronal function and the apparent propensity a subgroup of JdVS patients has for  
139 acute neuropsychiatric decompensation, we developed an induced pluripotent stem cell (iPSC)  
140 model and analyzed glutamatergic neurons and microglia by proteomics and  
141 phosphoproteomics.

142

## 143 **Methods**

### 144 **Subjects**

145 The JdVS patient is a male who was born full-term following an uncomplicated pregnancy who  
146 was diagnosed as a child following whole exome sequencing (WES), which revealed a typical  
147 *PPM1D* truncating mutation in exon 5 (c.1210C>T; p.Q404X). All *PPM1D* heterozygotes,  
148 whether patient-derived or developed using CRISPR-Cas9 editing (see below), will be referred

149 to as *PPM1D*<sup>+tr</sup>. Analysis of parental DNA showed that the mutation was de novo, as is the case  
150 for >90% of JdVS cases. His typically developing brother was used as one of the controls.  
151 Another typically developing control male was used to develop isogenic iPSC *PPM1D*<sup>+tr</sup> lines in  
152 which a truncating mutation was introduced in exon 5 using CRISPR-Cas9 gene editing (see  
153 **Additional file 1: Expanded Methods** for details). A third male was used as a typically  
154 developing control. These last two controls were characterized in another study (23).

155

### 156 **Development of iPSCs from peripheral blood CD34+ cells**

157 All methods used in this study are described briefly here; details can be found in **Additional file**  
158 **1: Expanded Methods**. iPSC lines were generated from human peripheral blood CD34+  
159 hematopoietic stem cells (HSC) with a CytoTune-iPS 2.0 Sendai Reprogramming Kit  
160 (Invitrogen) following the manufacturer's protocol, as previously described (24). All lines were  
161 capable of differentiating into the three germ layers and showed no expression of  
162 reprogramming transcription factors. Cytogenetic analysis was negative.

163

### 164 **CRISPR-Cas9 gene editing**

165 A heterozygous truncating variant in *PPM1D* exon 5 was generated by CRISPR-Cas9 gene  
166 editing, using a protocol described by Ran et al (25). Briefly, a guide RNA (gRNA) sequence  
167 coding for a region in exon 5 adjacent to a PAM sequence 9 base pairs from the patient  
168 mutation was chosen (**Figure 1: Additional file 1: Expanded Methods**).

169

### 170 **Differentiation of iPSCs into glutamatergic neurons**

171 iPSCs

172 were **Figure 1. DNA sequence analysis and Western blot of PPM1D truncating variants.**

173 maintained as previously described (23). Glutamatergic neuronal differentiation was induced

174 using a protocol developed by Zhang et al., in which differentiation is driven by overexpression

175 of the transcription factor NGN2 (26). A tet-inducible expression system was introduced and  
176 lentivirus particles prepared from the plasmid vectors; pLV\_TRET\_hNgn2\_UBC\_Puro (plasmid  
177 #61474) and FUdeltaGW-rtTA (plasmid #19780), followed by treatment with doxycycline and  
178 selection with puromycin (see **Additional file 1: Expanded Methods** for details). The protocol  
179 routinely leads to the production of a nearly pure culture of excitatory cortical glutamatergic  
180 neurons.

181

### 182 **Neurite outgrowth**

183 Neurite outgrowth was assessed blind to genotype using the NeuronJ plugin (27). Glutamatergic  
184 neurons were stained with Map2 and Tuj1 antibodies and imaged at 10x resolution. Images of  
185 patient and control neurons were converted to 8-bit grayscale, and individual dendrites were  
186 traced and labeled using the semiautomatic manual tracing tool. Approximately 10 images with  
187 an average of 12 neurons per field were analyzed per sample. The “measure tracings” function  
188 was used to determine mean length (in pixels) of the dendritic branches.

189

### 190 **Differentiation of iPSCs into microglia**

191 To generate microglia, we used kits from STEMCELL™ Technologies (STEMdiff™  
192 Hematopoietic Kit, catalog number 05310; STEMdiff™ Microglia Differentiation Kit, catalog  
193 number 100-0019; STEMdiff™ Microglia Maturation Kit, catalog number 100-0020) according to  
194 the manufacturer’s instructions, with minor modifications as described in **Additional file 1:**  
195 **Expanded Methods**. iPSCs are first differentiated into HSCs, followed by terminal  
196 differentiation into microglia. The microglia grow in suspension with the control and PPM1D<sup>+tr</sup>  
197 showing a similar morphology. (**Additional file 2: Fig. S1**).

198

### 199 **Fluorescence-activated cell sorting (FACS)**

200 Single-cell suspensions were used for flow cytometry staining. We followed a protocol for  
201 Staining Cell Surface Targets for Flow Cytometry from ThermoFisher. All antibodies were  
202 obtained from Stemcell Technologies, except for TMEM119, which is from Novus Biologicals.  
203 For HSCs, we used CD45 FITC (Catalog number 60018FI.1) CD43 APC (Catalog number  
204 60085AZ.1), and CD34 PE (Cat. 60013PE.1) antibodies. For microglia we used TMEM119 APC  
205 (Catalog FAB10313A) and CD11b PE (Catalog 60040PE.1) antibodies. Antibody concentrations  
206 were 5ul per 100ul for all Ab except TMEM119 for which 0.5ul per 100ul was used. Flow  
207 cytometry acquisition was obtained using a BD LSRII analyzer, and BD FlowJo software was  
208 used for data analysis.

209

### 210 **Cytokine array**

211 Microglia were seeded at  $5 \times 10^5$  cells/well in a 12 well, Matrigel-coated plate in STEMdiff  
212 Microglia Maturation media 24 days post differentiation. After 5 days of maturation, cells were  
213 stimulated with 100ng/ml LPS (O111:B4 strain; Sigma catalog # L4391) for 24 hours at 37°C.  
214 Supernatants were collected and analyzed using the Proteome Profiler Array Human Cytokine  
215 Array (R&D Systems catalog # ARY005B) following the manufacturer's instructions. Arrays were  
216 analyzed using Quick Spots Image Analysis Software. Each cytokine and chemokine on the  
217 array is measured in duplicate.

218

### 219 **Western Blotting**

220 Proteins were prepared with Pierce™ RIPA Buffer (Thermoscientific catalog # 89900) according  
221 to the manufacturer's protocol, with a protease inhibitor cocktail mix (Sigma catalog # P8340).  
222 Protein concentrations were verified using the BCA assay. Western Blotting was essentially  
223 carried out as previously described, with modifications, as described in **Additional file 1:**  
224 **Expanded Methods.** Phosphorylation of CaMKII (CaMK2) was analyzed by comparing the

225 phosphorylated and unphosphorylated proteins, which are also described in more detail in the  
226 expanded methods section.

227

## 228 **Proteomics and phosphoproteomics**

229 Proteomics and phosphoproteomics, and subsequent bioinformatics analyses were performed  
230 as previously described (28-35) (see **Additional file 1: Expanded Methods** for details)

231

## 232 **Results**

233

### 234 **Development of iPSCs**

235 A patient-specific line was developed from a male with JdVS who had a de novo nonsense  
236 mutation at codon 404 in exon 5 (c.1210C>T; p.Q404X) (**Figure 1**). The same mutation was  
237 found in one of the subjects in the original JdVS paper (individual 4) {{6152 Jansen,S. 2017}}.  
238 His typically developing brother was used as a control. We also used CRISPR-Cas9 gene  
239 editing on another control line to create truncating mutations in exon 5 near the patient's variant.  
240 Two clones with an "A" deletion 5 bp from the patient mutation were obtained. The deletion  
241 causes a frameshift and premature termination after 6 additional amino acids are inserted  
242 (c.1209delA; N402Ifs\*6). This is still within the boundaries of the most proximal truncating  
243 mutation described by Jansen et al., at cDNA position 1188 (4). Both the patient sample and the  
244 CRISPR-engineered lines show the truncated protein on a Western blot (**Figure 1**).

245

### 246 **Proteomics: glutamatergic neurons**

247 Proteomics and phosphoproteomics were carried out on glutamatergic neurons (day 21)  
248 differentiated from iPSCs. A total of four control and five PPM1D<sup>+tr</sup> samples were analyzed.  
249 4,948 proteins were detected among which 35 were significantly upregulated and 26 that were  
250 downregulated in the PPM1D<sup>+tr</sup> neurons (p<0.05, corresponds to a p-value of 4.32, see

251 **Additional file 3: Table S1**). The volcano plots for this analysis, as well as the subsequent  
252 proteomics and phosphoproteomics data described below are shown in **Figure 2**.  
253  
254 Gene Ontology (GO) analysis was carried out to characterize the pathways and processes  
255 affected by differentially expressed proteins (DEPs). The top GO pathway was, surprisingly,  
256 positive regulation of T cell differentiation (**Table 1; Additional file 3: Table S1**). This is  
257 probably due to expression of regulatory factors influenced by PPM1D that are expressed in  
258 both neurons and T-cells, an idea supported by the finding that DEPs contributing to the T cell  
259 differentiation GO term in neurons; CBFB, PNP, AP3D1, ANXA1, AP3B1, SART1, BAD,  
260 STAT5B, and ZMIZ1, are also expressed in peripheral blood mononuclear cell (PBMC) types  
261 and microglia (36). In addition, Ppm1d has been found to regulate T<sub>H</sub>9 cell development and T-  
262 cell differentiation in mice (37,38). Thus, the common regulation of these proteins in neurons  
263 and immune cells could be coincidental. The other top GO terms are related to the apparently  
264 novel effect of PPM1D on processing H/ACA snoRNAs, a class of small nucleolar RNAs  
265 (snoRNAs) that regulate ribosome biogenesis and alternative splicing (39).  
266  
267 We also analyzed neuronal DEPs by KEGG (Kyoto Encyclopedia of Genes and Genomes),  
268 which showed that the top pathway for upregulated proteins was spliceosome, consistent with  
269 the GO terms (**Table 2**). In addition, enrichment for proteins involved in several  
270 neurodegenerative disorders was also found (e.g., Amyotrophic Lateral Sclerosis [ALS],  
271 Huntington's Disease (HD), Parkinson's Disease (PD), Alzheimer's Disease (AD), and prion  
272 disease). The top differentially expressed down-regulated KEGG pathways were metabolic  
273 pathways, ribosomes, and, similar to the up-regulated pathways, ALS, PD, and HD. These  
274 findings suggest that features underlying the pathogenesis of JdVS are shared with those  
275 involved in some neurodegenerative disorders.

276

277 Analysis of the top individual up and down-regulated DEPs was particularly noteworthy for  
278 altered expression of proteins involved in ubiquitin signaling (**Table 3**). The top-upregulated  
279 protein, for example, was CUL4B, a scaffold protein of the CUL4B-Ring E3 ligase complex,  
280 which is expressed primarily in the nucleus where it plays a role in DNA repair and tumor  
281 progression (40-42). Loss of function (LOF) variants have been found in NDDs (43-46). CUL4B  
282 is also an immune regulator, and is involved in the degradation of SIN1, an mTORC2  
283 component (40,47-49).

284

285 Other ubiquitin signaling proteins among the top 10 upregulated DEPs were PJA2, an E3  
286 ubiquitin-protein ligase, and AUP1, which forms a complex with the ubiquitin-conjugating  
287 enzyme (E2), UBE2G2 (50-52). Among the top downregulated DEPs affecting ubiquitin  
288 signaling is PELI2, a member of the E3 ubiquitin ligase family that regulate the innate immune  
289 system by increasing NLRP3 inflammasome activation (53).

290

291 Other top upregulated DEPs of interest include SMARCE1, SLK, POFUT1, DKC1, and  
292 NEUROG2. SMARCE1 codes for an SWI/SNF chromatin remodeling complex component that  
293 regulates gene expression and can cause ASD when mutated (54-57).

294

295 Other proteins that were most downregulated in *PPM1D*<sup>+/-</sup> neurons were UPF2, NCAM2, TUB,  
296 and GSTZ1. UPF2 is a regulator of nonsense-mediated decay (NMD) and low expression is a  
297 factor in resistance to ATR inhibitors: ATR is a DNA damage sensor and a PPM1D substrate  
298 (9,58). Disruption of NMD has been associated with neurodevelopmental disorders (59) GSTZ1  
299 is a member of the glutathione S-transferase super-family that detoxifies products of oxidative  
300 stress, a process linked to PD, AD, and ALS (60-63).

301

302 **Phosphoproteomics: glutamatergic neurons**

303 Since PPM1D is a serine/threonine phosphatase, we also carried out a phosphoproteomics  
304 analysis on the samples used in the glutamatergic neuronal proteomics experiment. However,  
305 one sample was omitted for technical problems, so 4 control vs 4 *PPM1D*<sup>+/-tr</sup> neuronal samples  
306 were analyzed. A total of 7,542 phosphosites were detected (**Additional file 4: Table S2**). At  $p$   
307  $< 0.05$ , 174 differentially expressed phosphosites (DEPP) differed significantly between control  
308 and *PPM1D*<sup>+/-tr</sup> neurons; 46 were higher and 128 were lower. GO analysis showed that the most  
309 enriched phosphorylations are related to cytoskeleton organization, cellular component  
310 organization or biogenesis, and mRNA processing (**Table 1**). KEGG analysis of differentially  
311 expressed upregulated proteins showed that the top pathways were ErbB signaling, axon  
312 guidance, neurotrophin signaling, and regulation of the actin cytoskeleton (**Table 2**). Axon  
313 guidance and ErbB signaling were also among the top downregulated pathways, along with  
314 insulin signaling and spliceosome.

315

316 The top DEPP that increased in the *PPM1D*<sup>+/-tr</sup> neurons was SRRM1, which is involved in RNA  
317 processing, as a component of pre- and post-splicing multiprotein mRNP complexes that play  
318 major roles in RNA metabolism (**Table 3**) (63). Altered expression affects prostate cancer  
319 aggression and invasion of hepatocellular carcinoma cells (64,65). Mutations in *PPM1D*  
320 mutations are associated with both, suggesting that altered SRRM1 phosphorylation plays a  
321 role in *PPM1D*-associated cancers (68, 69). Strikingly, two phosphosites on SRRM1 (Ser725  
322 and Thr727) were also the top downregulated DEPPs. Predicted targets at Thr727 include  
323 HIPK1 and p38MAPK (<http://www.phosphonet.ca/>), which are *PPM1D* substrates. The findings  
324 suggest that regulation of SRRM1 is a novel feature of truncating *PPM1D* variants.

325

326 Interestingly, three of the top DEPPs were found in NUCKS1, a chromatin regulator that  
327 regulates DNA repair (66-68). NUCKS1 has been implicated in PD in genome wide association  
328 studies (GWAS) and is a known *PPM1D* substrate, although neither of the top three neuronal

329 NUCKS1 phosphosites occurs at SQ/TQ motifs, which are canonical PPM1D targets (9,69,70).  
330 Another protein that scored multiple hits among the top upregulated phosphosites is DCX  
331 (doublecortin), a cytoskeletal protein that stabilizes microtubules and regulates neuronal  
332 migration and cortical layering during development (71).

333

334 Differential phosphorylation of proteins that are known PPM1D substrates, such as ATM, CHK1,  
335 CHK2, and P53, were not detected, perhaps because the neurons were postmitotic and not  
336 subjected to conditions that would most effectively induce their phosphorylation (e.g., ionizing  
337 radiation). In fact, among the DEPPs that showed a decrease in phosphorylation expected of a  
338 PPM1D GOF effect, only three, ENAH, AKAP12, and ANK2 occurred at SQ sites, suggesting  
339 that the majority of neuronal DEPPs are secondary to the downstream effects of PPM1D on  
340 other kinases and phosphatases, although novel, noncanonical targets are possible as well.

341

342 Overall, the neuronal proteomics and phosphoproteomics data showed differential expression of  
343 proteins and phosphoproteins coregulated in T-cells, splicing, DDR, chromatin regulation,  
344 neurodegeneration, ErbB signaling, and ubiquitin ligases.

345

### 346 **Proteomics: Microglia**

347 As described in the introduction, we identified several JdVS cases in whom severe motor and  
348 behavioral regression occurred following infections and non-infectious stressors. Although these  
349 examples of acute neuropsychiatric decompensation appear to be rare occurrences in JdVS, we  
350 extended the proteomics analysis to include microglia. An additional rationale is that microglia  
351 have been implicated in the pathogenesis of ASD and NDD (72-75). Microglia were developed  
352 from six iPSC lines (three control and three *PPM1D*<sup>+tr</sup>). The differentiation protocol produced  
353 similar populations of TMEM119/CD11B double-positive cells; between 71.9 to 88% (**Figure 3**).

354 5,759 proteins were detected, which included 76 that were significantly upregulated and 76 that  
355 were downregulated (**Additional file 5: Table S3; Figure 2**). GO analysis showed enrichment  
356 of DEPs related to blood vessel development: aorta morphogenesis, blood vessel lumenization,  
357 and blood vessel morphogenesis, although the p-values are modest (**Table 4**). Nevertheless,  
358 these findings are of interest. The upregulated proteins that contributed to these GO findings,  
359 DLL4, RBPJ, and LRP, are all involved in endothelial function that can affect the brain-blood  
360 barrier (BBB) suggesting that *PPM1D* truncating mutations increase BBB permeability (76,77).  
361 In fact, *PPM1D* has been shown to be a BBB regulator (78). The findings support the idea that  
362 patients with JdVS are prone to neuroinflammation in response to a peripheral immune  
363 challenge.

364  
365 Also consistent with a neuroinflammatory phenomenon are the GO terms of enriched DEPs  
366 showing an effect on the production and positive regulation of NLRP3 inflammasome complex  
367 assembly. IL-18 is a proinflammatory cytokine produced, along with IL-1 $\beta$ , as a result of NLRP3  
368 inflammasome activation (79-81). However, the level of significance for this GO term is modest.

369  
370 The top pathway for upregulated proteins was lysosome, but similar to the KEGG analysis of  
371 neurons, among the top pathways for both up and downregulated proteins are  
372 neurodegenerative disorders. The lysosome pathway could indicate a predilection for disruption  
373 of autophagy, a process linked to neurodegenerative and neurodevelopmental disorders (**Table**  
374 **5**) (82-85). Interestingly, the most upregulated DEPs proteins in *PPM1D*<sup>+tr</sup> microglia are several  
375 regulators of ubiquitin signaling and innate immune pathways (**Table 6**). These included,  
376 CDC34, a Cullin-Ring E2 ubiquitin-conjugating enzyme, GBP5, a member of the GTPase  
377 subfamily induced by interferon-gamma (IFN- $\gamma$ ), CDBP2, a CD2 antigen cytoplasmic tail-binding  
378 protein that regulates T-cell activation and IL-2 production, KLHDC4, a member of the Kelch-like

379 proteins that act as substrate adaptors for Cullin 3 ubiquitin ligases, PELI1, an E3 ubiquitin-  
380 protein ligase pellino homolog that regulates NLRP3-induced caspase-1 activation and IL-1 $\beta$   
381 maturation, ZNFX1, which functions as a dsRNA sensor and regulator of antiviral responses,  
382 and TEP1, a telomerase protein component that can influence innate immune responses  
383 through cGAS/STING (cyclic GMP-AMP synthase-stimulator of interferon genes) activation, a  
384 cytosolic DNA sensor (86-92).

385  
386 Many of the most downregulated proteins are also involved in innate immunity including TANK,  
387 which activates NF- $\kappa$ B and cGAS-STING signaling, APOBEC3G, a cytidine deaminase involved  
388 in anti-viral innate immunity, and HERC6, an E3 ligase for ISG15 that regulates ISGylation, a  
389 post-translational modification induced by interferon that has ubiquitin-like, protein modifying  
390 effects (93-103).

391  
392 Another key downregulated protein is POGZ, a chromatin regulator that also promotes  
393 homology-directed DNA repair (104). LOF mutations are commonly found in ASD and NDD  
394 (105,106). POGZ binds to ADNP, and their deficiency in mice induces significant upregulation of  
395 genes enriched in neuroinflammation and altered microglial and glutamatergic neuronal function  
396 (105-108). LOF mutations in ADNP have been found in NDD and ASD (including regressive  
397 autism; see discussion) (109-111). Neither POGZ nor ADNP is significantly differentially  
398 expressed in glutamatergic neurons. These findings suggest that decreased POGZ expression  
399 in microglia is playing a role in the neurodevelopmental features of JdVS.

400

#### 401 **Phosphoproteomics: Microglia**

402 The phosphoproteomics analysis detected 3458 phosphosites of which only 4 showed a  
403 significant increase in the *PPM1D*<sup>+tr</sup> microglia, while 39 were significantly decreased  
404 (**Additional file 6: Table S4; Figure 2**). The top GO terms for differentially phosphorylated

405 proteins were related to RNA splicing, regulation of small GTPase signaling, chromatin  
406 remodeling, protein phosphorylation, cytoskeleton organization, and cellular response to DNA  
407 damage stimulus, and the top KEGG pathway was spliceosome, similar to the neuronal  
408 proteomics and phosphoproteomics studies (**Table 4**; **Table 5**). The top upregulated  
409 phosphorylated proteins in *PPM1D<sup>+tr</sup>* microglia were in PXN, DDX54, TOP2B, MACF1, CCNY,  
410 and SRRM1 (**Table 6**). Remarkably, this overlaps with the finding that SRRM1 was the top  
411 upregulated, as well as the top downregulated phosphorylated protein in *PPM1D<sup>+tr</sup>* neurons, as  
412 described above, providing additional support for the idea that PPM1D truncating mutations  
413 disrupt SRRM1 function. An increase in phosphorylation at S429 in both neurons and microglia  
414 was detected. This is predicted to be a substrate for the PIM family of kinases, which promote  
415 tumorigenesis and immune escape by HIV (112,113).

416  
417 Two phosphosites in TRAFD1 were among the top 10 DEPPs. TRAFD1 is a transcription factor  
418 that acts as a negative feedback regulator of the innate immune system to control excessive  
419 immune responses (114,115). A similar occurrence in microglia could perhaps be relevant to the  
420 acute neuropsychiatric decompensation that occurs in some JdVS patients.

421  
422 The most downregulated DEPPs were found in SERF2, FLI1, UFL1, SNX5, and VPS50. SERF2  
423 is small EDRK-rich factor 2 that modifies amyloid fiber assembly and promotes protein  
424 misfolding (116). FLI1 is a member of the ETS transcription factor family that is disrupted in  
425 Ewing Sarcoma and acute myelogenous leukemia (117). And UFL1 (UBiquitin-like modifier 1  
426 Ubiquitin-like modifier 1 ligating enzyme 1) is a regulator of UFM1 conjugation (UFMylation), a  
427 ubiquitin-like modification that plays a key role in maintaining cell homeostasis under cellular  
428 stress, including DDR (118-120). SNX5 is a component of an autophagosomal complex and  
429 VPS50 is an endosome-recycling protein (121,122).

430

431 In summary, the microglia proteomics and phosphoproteomics analyses suggest that reduced  
432 expression of POGZ is a candidate for the cognitive and behavioral aspects of JdVS, and that  
433 truncated PPM1D could disturb innate immune responses in the brain through altered regulation  
434 of ubiquitin signaling, DDR, splicing, altered expression or function of key genes, and perhaps  
435 BBB permeability.

436

### 437 **Proteomics Analysis of lipopolysaccharide (LPS)-activated microglia**

438 To test the hypothesis that PPM1D<sup>+tr</sup> microglia have an altered response to an innate immune  
439 system challenge, the effect of LPS was analyzed by proteomics. One hundred and fifty-eight  
440 proteins were upregulated in the PPM1D<sup>+tr</sup> samples, and 254 were downregulated.

441 **(Additional file 7: Table S5; Figure 2).** The top GO term was negative regulation of interleukin-  
442 6 (IL-6), a proinflammatory cytokine implicated in neuroinflammation, maternal immune  
443 activation, ASD, schizophrenia, and depression (**Table 7**) (123-126). However, the p-value was  
444 modest. KEGG analysis showed that the top pathways for upregulated proteins were lysosome,  
445 metabolic pathways, and several neurodegenerative disorders, similar to the findings in  
446 uninduced microglia and glutamatergic neurons (**Table 8**). Downregulated proteins were  
447 enriched for spliceosome, nucleocytoplasmic transport, and ALS, overlapping with other  
448 proteomics findings. Proteins involved in the response to several infectious diseases were also  
449 detected in the KEGG analysis.

450

451 Examination of individual DEPs showed striking patterns consistent with innate immune  
452 dysregulation, in particular, ubiquitin signaling (**Table 9**). The top upregulated protein in  
453 PPM1D<sup>+tr</sup> microglia was UHRF1BP1 (UHRF1-binding protein 1), which binds to UHRF1, a  
454 RING-finger E3 ubiquitin ligase, a regulator of Treg cell proliferation (127,128). Non-  
455 synonymous variants have been found in systemic lupus erythematosus (129). However, the  
456 effects of UHRF1BP1 and UHRF1 on microglia are not known. GBA1 catalyzes the cleavage of

457 glycosphingolipids—glucosylceramide and glucosyl sphingosine. Genetic variants are known risk  
458 factors for PD and Lewy Body Dementia, and biallelic LOF variants cause Gaucher disease  
459 (130-134). RAB11A is a member of the RAS family of small GTPases and is a regulator of toll  
460 receptor trafficking (134,135).

461

462 The most downregulated DEP was the ubiquitin protein ligase E3 component n-recognin 4  
463 protein, UBR4, which regulates oxidative stress by promoting K27-linked-ubiquitylation of N-  
464 terminal oxidized cysteines leading to proteasomal degradation (136). It's also a regulator of  
465 interferon signaling (137,138) and the proteasomal degradation of PINK1, which is involved in  
466 the pathogenesis of PD (see discussion) (138-140). *UBR4* variants have been linked to early-  
467 onset dementia (140). Other top-downregulated proteins include HAS1, a regulator of the  
468 extracellular matrix that is induced by LPS and KCTD5, a BTB/POZ domain-containing protein  
469 that functions as substrate-specific adaptor for Cullin3-based E3 ligases (141-143).

470

#### 471 **Phosphoproteomics LPS treated microglia**

472

473 Phosphoproteomics was carried out on the same samples used in the proteomics analysis. A  
474 total of 3,458 phosphosites were detected; 42 showed a significant increase in the LPS treated  
475 *PPM1D<sup>+tr</sup>* microglia, and 182 showed a significant decrease (**Additional file 8: Table S6;**  
476 **Figure 2**). Strikingly, four of the top seven phosphosites that increased in the LPS-stimulated  
477 *PPM1D<sup>+tr</sup>* microglia were in UBR4, although neither of the sites is a canonical PPM1D target  
478 motif (**Table 9**). The top phosphosite is at S2718, which is phosphorylated in UV irradiated cells,  
479 consistent with an effect of PPM1D or its substrates on DDR (144). This and the other top UBR4  
480 phosphosites have an SS motif. As noted above, UBR4 is also the most downregulated DEP in  
481 LPS-treated microglia, suggesting that UBR4 phosphorylation is inversely correlated with UBR4  
482 protein levels. There are also two enriched phosphosites in PLXNC1, a member of the plexin

483 family of transmembrane receptors for semaphorins, which are involved in brain development  
484 and immune responses (145). IL16 had the most differentially increased phosphosite after  
485 UBR4. It is a CD4+ immune cell-specific chemoattractant cytokine that has been implicated in  
486 multiple sclerosis (146,147).

487

488 The most downregulated phosphosite was in RASAL3, a RasGAP that is highly expressed in  
489 neutrophils. Deficiency enhances immune activation in acute inflammatory conditions (148). GO  
490 analysis of all differential phosphosites showed enrichment of phosphoproteins involved  
491 in RNA splicing, regulation of small GTPase-mediated signal transduction, chromatin  
492 remodeling, cytoskeleton organization, and cellular response to DNA damage stimulus  
493 (**Table 7**). These findings overlap with the uninduced microglia phosphoproteomics analysis.  
494 Alterations in microglia's cytoskeleton function could potentially cause problems with their  
495 migration or phagocytic potential.

496

497 The top KEGG pathways for phosphosites that increased in the *PPM1D*<sup>+tr</sup> microglia were Rap1  
498 signaling, Yesinia infection, platelet activation and regulation of cytoskeleton, while the terms  
499 spliceosome, regulation of actin cytoskeleton, viral life cycle (HIV-1) and thyroid hormone  
500 signaling pathway were pathways enriched with phosphosites that decreased in *PPM1D*<sup>+tr</sup>  
501 microglia (**Table 8**). A modest enrichment of phosphosites involved in ErbB signaling was also  
502 seen, which by itself seems relatively minor. However, in view of the enrichment of  
503 phosphosites in this pathway in neurons and uninduced microglia, as well as LPS-treated cells,  
504 the findings suggest that *PPM1D* truncating mutations can disrupt ErbB signaling. *PPM1D*  
505 expression has been found to affect breast cancer growth (149,150). In the brain, ErbB  
506 signaling plays a role in synaptic plasticity and has been implicated in NDD (151-154).

507

508 Overall, the findings show that immune stimulation of  $PPM1D^{+/tr}$  microglia results in altered  
509 expression of proteins involved in ubiquitin signaling, in particular, UBR4, actin cytoskeleton,  
510 RNA splicing, chromatin structure, and innate immune regulation, the latter of which could play  
511 a role in the decompensation some JdVS patients experience following infectious and non-  
512 infectious stressors.

513

514 In summary, the three cell types in which proteomics and phosphoproteomics were carried out  
515 (glutamatergic neurons, uninduced microglia, and LPS-stimulated microglia) showed several  
516 overlapping pathways: splicing, ubiquitin ligase expression, neurodegenerative disorders,  
517 chromatin organization, cytoskeleton dynamics, and ErbB signaling (**Figure 4**).

518

#### 519 **Functional analysis of glutamatergic neurons and microglia**

520 Most of the differentially expressed phosphosites in neurons and microglia were not at canonical  
521 SQ or TQ motifs recognized by PPM1D, so the GOF effect of truncated PPM1D could not be  
522 unequivocally validated using the phosphoproteomics data we obtained. Consequently, we  
523 examined a known neuronal PPM1D target, CaMKII T287 to confirm a GOF effect in neuronal  
524 cells. As shown in **Figure 5**, there was a statistically significant, 2-fold decrease in the relative  
525 expression of phospho-CAMKII in  $PPM1D^{+/tr}$  neuronal cells consistent with a GOF effect. Also  
526 shown in the figure, is a validation of the GO and KEGG findings that cytoskeleton function is  
527 disrupted in  $PPM1D^{+/tr}$  glutamatergic neurons; a significant decrease in neurite outgrowth was  
528 found. Cytoskeleton function is critical for neurite outgrowth and synapse development, and  
529 many ASD and NDD candidate genes have an adverse effect on these processes (155-157).

530

531 Finally, we measured the concentration of cytokines and chemokines in the supernatant  
532 following LPS treatment to assess microglia function following an innate immune challenge. The  
533 top GO term for LPS-treated  $PPM1D^{+/tr}$  microglia was negative regulation of IL-6. This was

534 based on DEPs that directly or indirectly affect IL-6 signaling (ZC3H12A, GBA, TNFAIP3,  
535 GAS6), rather than IL-6 levels per se, which was not detected in the proteomics analysis. As  
536 seen in **Figure 5C**, IL-6 was induced in LPS-treated control microglia, but not in the *PPM1D*<sup>+tr</sup>  
537 cells as predicted. However, because of a large standard error and the small sample size, the  
538 induction was not statistically significant. In addition, we detected a slight increase in baseline  
539 IL-18 levels in *PPM1D*<sup>+tr</sup> microglia compared with the controls, as predicted from the GO  
540 analysis, but that difference was also not statistically significant. There was also a decrease in  
541 IL-18 induction by LPS detected in the *PPM1D*<sup>+tr</sup> microglia compared with LPS-treated controls,  
542 but the difference fell short of statistical significance (p=0.2). This is consistent with the  
543 proteomics data, which showed a statistical trend towards a decrease in IL-18 in the *PPM1D*<sup>+tr</sup>  
544 LPS-treated microglia (-log<sub>2</sub> p-value of 3.79 = 0.07, see **Additional file 7: Table S5**). In  
545 addition, there was, somewhat unexpectedly, a significant decrease in the induction of the  
546 chemokines CCL2 and CCL3/CCL4 by LPS between the control and *PPM1D*<sup>+tr</sup> microglia (p=  
547 0.0009 and 0.02, respectively. In fact, while LPS induced an increase in CCL2 in the control  
548 sample that showed a trend towards statistical significance (p=0.065), a significant decrease  
549 was detected in the *PPM1D*<sup>+tr</sup> cells (p=0.01). The findings suggest that truncated PPM1D  
550 causes deregulation of cytokine release.

551

## 552 **Discussion**

553 Although the sample size in this study was small, a number of interesting findings emerged that  
554 could explain the clinical features seen in JdVS. One is the significant decrease in the  
555 expression of the chromatin regulator and high-confidence ASD candidate gene *POGZ* in  
556 *PPM1D*<sup>+tr</sup> microglia. This is consistent with the finding that *Pogz* KO mice show an upregulation  
557 of genes enriched in neuroinflammation and an increase in microglia phagocytosis in the  
558 prefrontal cortex (105). Similar and overlapping findings were found in *Adnp* KO mice. *ADNP* is  
559 another high-confidence ASD gene that forms a nuclear complex with *POGZ* and was also

560 decreased in *PPM1D*<sup>+tr</sup> microglia (108). Given the findings in mouse *Pogz* KO models, the  
561 significant decrease of POGZ in *PPM1D*<sup>+tr</sup> suggests that microglia are playing a direct role in  
562 the neurodevelopmental aspects of JdVS. However, considering the neuronal proteomics  
563 analysis, neurons are likely also playing a causal role, as expected of a gene like *PPM1D* that is  
564 expressed ubiquitously throughout the CNS in neurons and non-neuronal cells. Considering that  
565 *PPM1D* is expressed at much higher levels in the cerebellum compared to other brain regions,  
566 as are both *POGZ* and *ADNP*, it will be particularly important to carry out the studies reported  
567 here in cerebellar organoids derived from our iPSC lines, or in mouse models. The cerebellum  
568 is now known to play a role in cognitive function and the development of ASD and NDD, in  
569 addition to its well-established effects on locomotor function and coordination (158-160).  
570

571 Another interesting aspect of this study is related to the clinical observation that a small  
572 proportion of JdVS patients have acute neuropsychiatric decompensation, a phenomenon that  
573 has been described in genetic subgroups of NDD and ASD (109,161-164). One of the patients  
574 presented with symptoms consistent with PANS, as we previously reported (15), and two others  
575 with acute and subacute behavioral and motor regression following infection and noninfectious  
576 stressors (unpublished observations). PANS is an autoinflammatory/autoimmune disorder  
577 induced by group A beta-hemolytic *Streptococcus* and other infectious microbes, and behavioral  
578 regression in ASD has been hypothesized to have immune-based or infection-triggered  
579 underlying pathogenesis in some cases (162,165-167). Interestingly, *ADNP* is one of 11 ASD-  
580 associated candidate genes, most commonly found in regressive ASD (109). Our microglia  
581 proteomics and phosphoproteomics findings support the idea that *PPM1D* truncating mutations  
582 can affect the susceptibility to immune-based decompensation. For example, the microglia GO  
583 analysis showed that proteins involved in endothelial function that can affect the BBB are  
584 differentially expressed; disruption of the BBB resulting in increased permeability to peripheral  
585 inflammatory cytokines, chemokines, complement, and immune cells, has been viewed as a

586 pathogenic feature of neuroinflammatory and neurodegenerative disorders (168-171). Also  
587 consistent with a neuroinflammatory vulnerability are the various connections to dysregulated  
588 innate immunity we detected in *PPM1D*<sup>+/-</sup> microglia, primarily through altered expression of  
589 ubiquitin ligases and ubiquitin-conjugating enzymes. Most notable is UBR4, which was the most  
590 downregulated DEP in LPS-stimulated microglia. UBR4 was also among the most down-  
591 regulated proteins detected in *PPM1D*<sup>+tr</sup> microglia treated with poly I:C and IL-17 (unpublished  
592 observations, manuscript in preparation). As noted in the results section, UBR4 regulates  
593 oxidative stress and interferon signaling, and the degradation of PINK1, a mitochondrial  
594 serine/threonine kinase that recruits the E3 ligase PARKIN (PRKN) to induce mitophagy (136-  
595 138,172). Homozygous, LOF mutations in either *PINK1* or *PRKN* are found in early onset,  
596 autosomal recessive forms of PD (139,140). Interestingly, we are aware of two cases of acute  
597 neuropsychiatric decompensation consistent with PANS who are heterozygous for LOF  
598 mutations in *PRKN* (manuscript in preparation). This connection between LPS-stimulated  
599 *PPM1D*<sup>+tr</sup> microglia and PD suggests a common vulnerability to environmental stressors due to  
600 dysfunctional UBR4 signaling, with subsequent adverse effects on proteasomal degradation and  
601 mitophagy. A defect in mitophagy homeostasis has been implicated in the pathogenesis of PD,  
602 as well as AD (173,174). *UBR4* variants have been found in some families with early-onset  
603 dementia (175). The effect of *PPM1D* truncating mutations on mitophagy has not yet been  
604 carried out. It should be noted that DEPs aside from UBR4 are connected to PD as seen in the  
605 KEGG pathway analyses showing that PD (and other neurodegenerative disorders) is among  
606 the top GO and KEGG pathways in both neurons and microglia.

607

608 In addition to UBR4, a number of other E3 ubiquitin ligases and their regulators, and ubiquitin-  
609 conjugating enzymes involved in innate immune responses were among the most differentially  
610 expressed proteins in untreated *PPM1D*<sup>+tr</sup> microglia (CDC34, KLHDC4, and PELI1;  
611 upregulated: HERC6; downregulated), and in LPS stimulated microglia (UHRF1BP1,

612 upregulated), as noted in the results section. In addition, the top-upregulated protein in  
613 *PPM1D*<sup>+tr</sup> neurons was CUL4B, a component of the CUL4B-Ring E3 ligase. The specific  
614 substrates affected by these ubiquitin regulators in microglia and neurons, and how they might  
615 be involved in JdVS and neuroinflammation need to be investigated.

616

617 An important finding to consider regarding the neuroinflammatory potential of *PPM1D*<sup>+tr</sup>  
618 microglia is the seemingly paradoxically lack of induction of IL-6 following LPS stimulation and  
619 the GO analysis that showed an enrichment of proteins that negatively regulate IL-6. This  
620 cytokine is one of the major proinflammatory cytokines implicated in neuroinflammation and  
621 maternal immune activation (123,176,177) In fact, in addition to IL-6, there was a generalized  
622 blunting of LPS-mediated cytokine induction in *PPM1D*<sup>+tr</sup> microglia (**Figure 5C**). This was  
623 particularly the case for CCL2 and CCL3/CCL4, which showed significant decreases compared  
624 with LPS-induced control microglia. A blunted induction of ICAM-1 and IL-8 was also detected,  
625 but the control vs *PPM1D*<sup>+tr</sup> difference was only significant for the latter (p=0.05). This suggests  
626 that TLR4 signaling is attenuated by truncated PPM1D. These findings need to be validated in a  
627 larger iPSC dataset, which is currently being carried out, and animal models. Reduced  
628 expression of CCL2 and CCL3/CCL4, which are potent monocyte attractants, in response to  
629 LPS activation, could affect the recruitment of transmigrating monocytes, a population of  
630 peripheral monocytes that can cross the BBB (178,179). Considering the dichotomy of  
631 monocytes and macrophages into pro- and anti-inflammatory subtypes, the effect of the blunted  
632 activation of CCL2 and CCL3/CCL4 on a neuroinflammatory process is difficult to predict and  
633 would need to be evaluated in an animal model. Furthermore, if the connection between  
634 *PPM1D* GOF variants and neuroinflammation is confirmed, then the idea that cytokines and  
635 chemokines affecting microglia and brain function are mediators may be too limiting. In the case  
636 of truncated PPM1D, a disturbance in microglia homeostasis and function may be at play, rather  
637 than an excessive release of proinflammatory cytokines and chemokines.

638

639 It is important to note that the iPSC lines used in these studies were not made from subjects  
640 with acute psychiatric decompensation, in either the JdVS subject we used or, especially, the  
641 CRISPR lines, which were made from a typically developing control. Thus, while connections to  
642 a neuroinflammatory process in this study are based on differences between control and  
643 *PPM1D* truncating mutations, they are occurring in the context of cellular stress conditions  
644 inherent in growing cultured cells in artificial media in an incubator. Therefore, replication in an  
645 animal model is essential.

646

647 Finally, it is important to consider the microglia findings in the context of the increased infections  
648 that occur in some JdVS children. In the original report of 14 cases, and a subsequent follow up  
649 of 33 cases, recurrent infections, in particular otitis media, were reported in approximately half  
650 (1,4). Although this has not been evaluated systematically, the increase in infections seen in  
651 some children has been sufficiently severe to warrant evaluations for immunodeficiencies by  
652 their physicians, which have been non-diagnostic so far. Considering the physiological and  
653 functional overlap between microglia and peripheral monocytes/macrophages, the differential  
654 expression of proteins involved in immune responses that were found in our proteomics  
655 analysis, as well as the blunted effect on cytokine and chemokine release could be having a  
656 similar effect in the periphery, reducing the effectiveness of an innate immune response to  
657 infections.

658

### 659 **Limitations**

660 The small sample size was a major limitation. Another is extrapolating data related to  
661 neuroinflammation using an in vitro microglia differentiation and cell culture system that is  
662 probably inducing cellular stress.

663

664 **Conclusion**

665 In summary, our findings show plausible mechanisms for the neurodevelopmental and cognitive  
666 features of JdVS, as well as the increased risk of neuroinflammatory-mediated decompensation,  
667 and perhaps the increased rate of infections seen in patients. The mechanistic links we  
668 identified to regression in NDD are also significant. Our findings provide additional support for  
669 the idea that a subgroup of NDD and ASD cases can experience neuropsychiatric  
670 decompensation caused by dysregulated innate immunity that is potentially treatable with  
671 immune modulators, as suggested by other investigators (162,180). In addition, the molecular  
672 connection to PD found with UBR4 and other DEPs (e.g., NUCKS1, GBA1) could also be  
673 significant in that unrecognized and under-treated neuroinflammatory processes could pose a  
674 future risk of PD and other neurodegenerative disorders. Thus, our analysis of JdVS, a rare  
675 disease with fewer than 100 reported cases, could be informative for disorders that have greater  
676 public health significance.

677

678 **Abbreviations**

679 JdVS (Jansen de Vries Syndrome)  
680 iPSC (induced pluripotent stem cell)  
681 LOF (loss-of-function)  
682 GOF (gain of function)  
683 LPS (lipopolysaccharide)  
684 NDD (neurodevelopmental disorder)  
685 ADHD (attention deficit hyperactivity disorder)  
686 ASD (autism spectrum disorder)  
687 DDR (DNA damage response)  
688 OCD (obsessive-compulsive disorder)  
689 KO (knockout)

690 hSC (hematopoietic stem cells)  
691 FACS (Fluorescence-activated cell sorting)  
692 PANS (pediatric acute-onset neuropsychiatric syndrome)  
693 GO (Gene Ontology)  
694 KEGG (Kyoto Encyclopedia of Genes and Genomes)  
695 BBB (brain blood barrier)  
696 ALS (Amyotrophic Lateral Sclerosis)  
697 HD (Huntington Disease)  
698 PD (Parkinson Disease)  
699 AD (Alzheimer Disease)  
700 IFN- $\gamma$  (interferon-gamma)  
701 cGAS/STING (cyclic GMP-AMP synthase-stimulator of interferon genes)

702

### 703 **Declarations**

### 704 **Ethics approval and consent to participate**

705 Informed consent was obtained by the corresponding author under an Albert Einstein College of  
706 Medicine, IRB-approved protocol.

707

### 708 **Consent for publication**

709 Consent for publication was obtained from participants and parents

710

### 711 **Availability of data and materials**

712 Proteomics and phosphoproteomics data were deposited at xxxxxxxxxx ().

713

### 714 **Competing interests**

715 The authors have no competing interests

716

## 717 **Funding**

718 HML is supported by the NIH/NIMH (R21 MH131740) and the NIH/NICHD (P30 HD071593) to  
719 the Albert Einstein College of Medicine's Rose F. Kennedy Intellectual and Developmental  
720 Disabilities Research Center. The Lachman lab also receives support from the Janice C.  
721 Blanchard Family Fund, The iPS Cell Research for Ryan Stearn fund. The Sidoli lab gratefully  
722 acknowledges funding from the Einstein-Mount Sinai Diabetes center, Merck, Relay  
723 Therapeutics, Deerfield (Xseed award), and the NIH Office of the Director (S10OD030286). The  
724 Cytex® Aurora System - Full Spectrum Flow Cytometry unit was supported by an NIH  
725 instrument grant, S10 OD026833. The Albert Einstein College of Medicine National Cancer  
726 Institute center grant, P30CA013330, provided support for the FACS facility

727

## 728 **Authors' contributions**

729 JTA (proteomics and phosphoproteomics, bioinformatics)  
730 EP (prepared iPSCs, differentiated neurons and microglia, proofread manuscript, FACS)  
731 HD (Western blots)  
732 RNB (Western blots)  
733 JB (Neurite outgrowth)  
734 JZ (FACS)  
735 SS (proteomics and phosphoproteomics, bioinformatics)  
736 HML (conceived and designed experiment, analyzed data, wrote manuscript)

737

## 738 **Acknowledgments**

739 We want to thank the Jansen de Vries Syndrome Foundation for their work and the families who  
740 provided samples for iPSC development. We also want to thank the Human Pluripotent Stem

741 Cell Core (Director Eric Bouhassira, and Zi Yan) at the Albert Einsein College of Medicine for  
742 preparing and characterizing iPSC lines.

743

#### 744 **Figure and Table Legends**

745 **Figure 1. DNA sequence analysis and Western blot of PPM1D truncating variants.** A. Map  
746 of PPM1D showing the 6 exons with the catalytic domain depicted as a solid bar. The two  
747 clusters of JdVS mutations are in the 3'-end of exon 5 and the 5'-end of exon 6. B. DNA  
748 sequence strip of wild type allele on top and the patient sample showing the c.1210C>T;  
749 p.Q404X nonsense mutation on bottom. The region covered by the guide RNA used for  
750 CRISPR-Cas 9 engineering is shown. C. Two isogenic lines with an "A" deletion were generated  
751 with CRISPR. D. PPM1D Western blot showing wild-type protein and the truncated protein.  
752 Cyclophilin is a loading control. Lanes 1 and 2 are control samples, lane 3 is the patient sample,  
753 and lanes 4 and 5 are two CRISPR lines.

754

755 **Figure 2. Volcano plots of differentially expressed proteins and phosphoproteins for all**  
756 **analyses.** -log<sub>2</sub> value of 4.32 corresponds to p=0.05, which is the cutoff.

757

758 **Figure 3. FACS analysis of microglia.** Microglia were developed from three control iPSC lines  
759 (PPM60C, LS200, and LS400), and three patient lines (PPMOOD, 36C, 36E). PPM60C is the  
760 typically developing sibling control of PPMOOD, and LS200 is the isogenic control for 36C and  
761 36E. LS400 is another typically developing control. Cells were sorted using conjugated  
762 antibodies against the microglia markers TMEM119 and CD11b, the latter of which also binds to  
763 macrophages. Microglia are positive for both double-positive cells.

764

765 **Figure 4. Summary of neuronal and microglia proteomics and phosphoproteomics.** Six  
766 pathways (center of each block, light grey) were found by either GO or KEGG (up or

767 downregulated) that were shared in three or more of the six different conditions analyzed in this  
768 study; proteomics and phosphoproteomics on glutamatergic neurons, untreated microglia, and  
769 LPS induced microglia (shared dark grey block; not shared, white block)

770

771 **Figure 5. CaMKII, Neurite Outgrowth, Cytokine Release. A.** CaMKII phosphorylation was  
772 analyzed by quantifying Western blot signals for CaMKII, phospho-CaMKII, and cyclophilin as a  
773 loading control. The graph in 5A is a plot of the ratio of the normalized phospho-CaMKII signal  
774 (relative to cyclophilin) divided by the normalized CaMKII signal. A total of 4 control and 5  
775 *PPM1D<sup>+tr</sup>* neuronal samples were analyzed. The graph is the mean for the two groups, +/-  
776 SEM. The decrease in CaMKII phosphorylation was highly significant ( $p=0.0005$ , Student's t-  
777 test, two-tailed). **B.** Neurite outgrowth was measured in day 21 glutamatergic neurons as  
778 described in the methods section. Tracings from two control and two *PPM1D<sup>+tr</sup>* day 21  
779 glutamatergic neurons were obtained, blind to genotype, for a total of 400 and 229 neurons  
780 analyzed, respectively. The difference between the two was highly significant (mean +/- SEM,  
781  $8.9E-07$ , Student's t-test, two-tailed). **C.** Cytokine release was assayed using the Proteome  
782 Profiler Array Human Cytokine Array, as described in the methods. A total of 4 control and 3  
783 *PPM1D<sup>+tr</sup>* microglia samples were analyzed (the same samples that were analyzed in the  
784 proteomics and phosphoproteomics analyses plus an additional control that was not analyzed  
785 by proteomics. Culture supernatants were harvested after 24 hours of LPS treatment. Untreated  
786 (no tx) cells from the same differentiation were harvested simultaneously. The data are the  
787 means of 4 vs 3, with each spot on the array measured in duplicate. A Student's t-test was used  
788 to calculate statistical significance. Those at  $p < 0.05$  are indicated by asterisks: CCL2,  
789 untreated control LPS vs *PPM1D<sup>+tr</sup>* LPS ( $p=0.01$ ); untreated *PPM1D<sup>+tr</sup>* vs *PPM1D<sup>+tr</sup>* LPS  
790 ( $p=0.0009$ ) (note CCL2 control vs control LPS had a p-value of 0.065); CCL3/CCL4, untreated  
791 control vs control LPS ( $p=0.02$ ); CCL3/CCL4, control LPS vs *PPM1D<sup>+tr</sup>* LPS ( $p=0.02$ ); ICAM-1

792 untreated control vs control LPS ( $p=0.05$ ); IL-8, untreated control vs control LPS ( $p=0.02$ ),  
793 control LPS vs *PPM1D*<sup>+tr</sup> LPS ( $p=0.05$ );

794

795 **Table 1. Gene Ontology (GO) analysis, neurons.** All differentially expressed proteins and  
796 phosphoproteins were used to determine GO terms. Only the most significant terms are shown.  
797 For the complete list, see **Additional file 3: Table S1. Tab1.**

798

799 **Table 2. KEGG analysis, neurons.** KEGG analysis based on differentially expressed up-  
800 regulated proteins and phosphoprotein, and differentially expressed down-regulated proteins  
801 and phosphoproteins. See **Additional file 3: Table S1** for complete lists.

802

803 **Table 3. Differentially expressed proteins and phosphoproteins, neurons.** Differentially  
804 expressed up and down-regulated proteins and phosphoproteins based on total scores  
805 (calculated by multiplying Fold Change by the p-value [-log 2 of 4.32 corresponds to  $p=0.05$ ]).  
806 DEPs shown in descending order.

807

808 **Table 4. Gene Ontology (GO) analysis, microglia.** All differentially expressed proteins and  
809 phosphoproteins were used to determine GO terms. Only the most significant terms are shown.  
810 For the complete list, see **Additional file 5: Table S3.**

811

812 **Table 5. KEGG analysis, microglia.** Shows lists of the most significant KEGG pathways for up  
813 and downregulated proteins and phosphoproteins in *PPM1D*<sup>+tr</sup> microglia. See **Additional file 5:**  
814 **Table S3** for complete lists.

815

816 **Table 6. Differentially expressed proteins and phosphoproteins, uninduced microglia.**

817 Differentially expressed up and down-regulated proteins and phosphoproteins in baseline,  
818 untreated microglia.

819

820 **Table 7. Gene Ontology (GO) analysis, LPS induced microglia.** All differentially expressed

821 proteins and phosphoproteins were used to determine GO terms. Only the most significant

822 terms are shown. For the complete list, see **Additional file 7: Table S5.**

823

824 **Table 8. KEGG analysis, LPS treated microglia.** Differentially expressed up and down-

825 regulated proteins and phosphoproteins in baseline, untreated microglia. **Additional file 7:**

826 **Table S5.**

827

828 **Table 9. Differentially expressed proteins and phosphoproteins, LPS-treated microglia.**

829 Shows the top up and downregulated proteins and phosphoproteins in baseline, untreated

830 microglia. See **Additional file 7: Table S5 and Additional file 8: Table S6** for all proteins and

831 phosphoproteins.

832

833 **Additional Files**

834 **Additional file 1: Expanded Methods.** This file contains a detailed description of the methods

835 used in this study.

836

837 **Additional file 2: Fig. S1.** Microscopic image of unstained microglia grown in suspension. Two

838 controls and two *PPM1D*<sup>+tr</sup> samples are shown. The bar is 200  $\mu$ M. Two other samples not

839 available.

840

841 **Additional file 3: Table S1. Neuron proteomics, PPM1D<sup>+tr</sup> vs controls. Tab 1. Gene**  
842 **Ontology (GO) analysis.** Control sample names on top are shown in pastel; 1 and 4, 2 and 3  
843 are biological duplicates. PPM1D<sup>+tr</sup> samples are shown in light green. Samples 1 and 2, as well  
844 as 3 and 5, are biological duplicates. Differentially expressed proteins are arranged in  
845 descending order based on highest to lowest scores in a comparison of all PPM1D<sup>+tr</sup> samples  
846 vs all controls. The score is calculated by multiplying Fold Change by the p-value (-log 2 of 4.32  
847 corresponds to p=0.05). **Tabs 2 and 3** (Neuron PPM1D<sup>+tr</sup> Up KEGG and Neuron PPM1D<sup>+tr</sup>  
848 Down KEGG, respectively) shows the KEGG analysis of all proteins that increased and  
849 decreased in the *PPM1D*<sup>+/-</sup> samples.

850

851 **Additional file 4: Table S2. Neuron phosphoproteomics, PPM1D<sup>+tr</sup> vs controls.** Control  
852 sample names on top are shown in pastel. Controls 1 and 3, and 2 and 4 are biological  
853 duplicates. PPM1D<sup>+/-</sup> sample names are shown in green. Samples 2 and 4 are biological  
854 duplicates. Tab 1, DEPPs are differentially expressed phosphoproteins arranged in descending  
855 order based on highest to lowest scores, as described in the legend for Additional file 3: Table  
856 S1. Tab 1 (Phosphosites and GO) contains all phosphorylated proteins in descending order and  
857 the GO analysis. Tab 2 (normalize to protein value) show GO analysis and volcano plot. Tabs 3  
858 and 4 are neuron phospho up 500 EnrichR and neuron phospho down 500 EnrichR,  
859 respectively, showing KEGG pathway analysis for phosphoproteins that increase or decrease in  
860 PPM1D<sup>+/-</sup> neurons. Additional GO analyses for up and down regulated phosphoproteins are  
861 shown, but were not described in the paper in order to avoid redundancy.

862

863 **Additional file 5: Table S3. Microglia proteomics, PPM1D<sup>+tr</sup> vs controls.** Three control  
864 samples and three PPM1D<sup>+/-</sup> samples were analyzed. The microglia were in their baseline state  
865 – no treatment (no tx). Tab 1 (processing) shows the detailed steps of data processing starting  
866 from raw abundance to log2 transformation, to normalization and to imputation of missing

867 values. Tab 2 is the differentially expressed protein list calculated as described in the neuron  
868 proteomics analysis (see figure legend, Additional file 3: Table S1), along with the GO analysis.  
869 Tab 3 is the DAVID KEGG analysis of up regulated proteins, which was not discussed in the  
870 paper since it overlapped with other findings. Tabs 4 and 5 are the KEGG pathways for the up  
871 and down regulated proteins, respectively, using 500 EnrichR. Tab 6 is the DAVID KEGG  
872 analysis of up regulated proteins.

873

874 **Additional file 6: Table S4; Figure 2. Microglia phosphoproteomics, PPM1D<sup>+tr</sup> vs controls.**

875 Phosphoproteomics was carried out on the same samples described in Additional file 5: Table  
876 S3. Tab 1 (PPM1D+tr untreated vs Control) contains the differentially expressed  
877 phosphoprotein list, along with the GO analysis. Tabs 2 and 3 (PPM1D+tr untreated Up KEGG  
878 and PPM1D+tr untreated Down KEGG) show KEGG pathways for up and downregulated  
879 phosphosites, respectively.

880

881 **Additional file 7: Table S5. LPS treated microglia proteomics, PPM1D<sup>+tr</sup> vs controls.**

882 Microglia derived from the same iPSC lines as described in the legend of Additional file 5: Table  
883 S3 were treated with LPS (see main text). Tab 1 (processing), as described in Additional file 5:  
884 Table S3. Tab 2 (microglia proteomics LPS) shows differentially expressed protein arranged by  
885 total score in descending order (PPM1D<sup>+tr</sup> vs controls) and GO analysis. KEGG pathway  
886 analysis for up and downregulated proteins are shown in Tabs 3 and 4, respectively (Microglia  
887 LPS Up KEGG; Microglia LPS down KEGG).

888

889 **Additional file 8: Table S6. LPS treated microglia phosphoproteomics, PPM1D<sup>+tr</sup> vs**

890 **controls.** Phosphoproteomics was carried out on LPS treated microglia using the same  
891 samples described in Additional file 7: Table S5. Tab 1 (PPM1D+tr LPS vs Cont LPS) shows  
892 differentially phosphorylated phosphosites arranged by total score in descending order and the

893 GO analysis. Tabs 2 and 3 (*PPM1D*<sup>tr</sup> LPS enriched Up KEGG; *PPM1D*<sup>tr</sup> LPS enriched Down  
894 KEGG) show the KEGG pathway analyses for phosphosites that increase or decreased,  
895 respectively.

896

897

898

## 899 References

900

901 (1) Wojcik MH, Srivastava S, Agrawal PB, Balci TB, Callewaert B, Calvo PL, et al. Jansen-de  
902 Vries syndrome: Expansion of the PPM1D clinical and phenotypic spectrum in 34 families. *Am J*  
903 *Med Genet A* 2023 Jul;191(7):1900-1910.

904 (2) Porrmann J, Rump A, Hackmann K, Di Donato N, Kahlert AK, Wagner J, et al. Novel  
905 truncating PPM1D mutation in a patient with intellectual disability. *Eur J Med Genet* 2019  
906 Jan;62(1):70-72.

907 (3) Lelieveld SH, Reijnders MR, Pfundt R, Yntema HG, Kamsteeg EJ, de Vries P, et al. Meta-  
908 analysis of 2,104 trios provides support for 10 new genes for intellectual disability. *Nat Neurosci*  
909 2016 Sep;19(9):1194-1196.

910 (4) Jansen S, Geuer S, Pfundt R, Brough R, Ghongane P, Herkert JC, et al. De Novo  
911 Truncating Mutations in the Last and Penultimate Exons of PPM1D Cause an Intellectual  
912 Disability Syndrome. *Am J Hum Genet* 2017 Apr 6;100(4):650-658.

913 (5) Kleiblova P, Shaltiel IA, Benada J, Sevcik J, Pechackova S, Pohlreich P, et al. Gain-of-  
914 function mutations of PPM1D/Wip1 impair the p53-dependent G1 checkpoint. *J Cell Biol* 2013  
915 May 13;201(4):511-521.

916 (6) Kahn JD, Miller PG, Silver AJ, Sellar RS, Bhatt S, Gibson C, et al. PPM1D-truncating  
917 mutations confer resistance to chemotherapy and sensitivity to PPM1D inhibition in  
918 hematopoietic cells. *Blood* 2018 Sep 13;132(11):1095-1105.

919 (7) Dudgeon C, Shreeram S, Tanoue K, Mazur SJ, Sayadi A, Robinson RC, et al. Genetic  
920 variants and mutations of PPM1D control the response to DNA damage. *Cell Cycle* 2013 Aug  
921 15;12(16):2656-2664.

922 (8) Bhattacharya D, Hiregange D, Rao BJ. ATR kinase regulates its attenuation via PPM1D  
923 phosphatase recruitment to chromatin during recovery from DNA replication stress signalling. *J*  
924 *Biosci* 2018 Mar;43(1):25-47.

- 925 (9) Gräf JF, Mikicic I, Ping X, Scalera C, Mayr K, Stelzl LS, et al. Substrate spectrum of PPM1D  
926 in the cellular response to DNA double-strand breaks. *iScience* 2022 Aug 9;25(9):104892.
- 927 (10) Cardoso M, Paulo P, Maia S, Teixeira MR. Truncating and missense PPM1D mutations in  
928 early-onset and/or familial/hereditary prostate cancer patients. *Genes Chromosomes Cancer*  
929 2016 Dec;55(12):954-961.
- 930 (11) Pechackova S, Burdova K, Macurek L. WIP1 phosphatase as pharmacological target in  
931 cancer therapy. *J Mol Med (Berl)* 2017 Jun;95(6):589-599.
- 932 (12) Li K, Liu Y, Xu S, Wang J. PPM1D Functions as Oncogene and is Associated with Poor  
933 Prognosis in Esophageal Squamous Cell Carcinoma. *Pathol Oncol Res* 2018 Oct 30.
- 934 (13) Alzahrani AS, Murugan AK, Qasem E, Alswailem MM, AlGhamdi B, Moria Y, et al. Absence  
935 of EIF1AX, PPM1D, and CHEK2 mutations reported in Thyroid Cancer Genome Atlas (TCGA)  
936 in a large series of thyroid cancer. *Endocrine* 2018 Sep 29.
- 937 (14) Nomura M, Mukasa A, Nagae G, Yamamoto S, Tatsuno K, Ueda H, et al. Distinct  
938 molecular profile of diffuse cerebellar gliomas. *Acta Neuropathol* 2017 Dec;134(6):941-956.
- 939 (15) Trifiletti R, Lachman HM, Manusama O, Zheng D, Spalice A, Chiurazzi P, et al.  
940 Identification of ultra-rare genetic variants in pediatric acute onset neuropsychiatric syndrome  
941 (PANS) by exome and whole genome sequencing. *Sci Rep* 2022 Jun 30;12(1):11106-3.
- 942 (16) Vreeland A, Thienemann M, Cunningham M, Muscal E, Pittenger C, Frankovich J.  
943 Neuroinflammation in Obsessive-Compulsive Disorder: Sydenham Chorea, Pediatric  
944 Autoimmune Neuropsychiatric Disorders Associated with Streptococcal Infections, and Pediatric  
945 Acute Onset Neuropsychiatric Syndrome. *Psychiatr Clin North Am* 2023 Mar;46(1):69-88.
- 946 (17) Chang K, Frankovich J, Cooperstock M, Cunningham MW, Latimer ME, Murphy TK, et al.  
947 Clinical evaluation of youth with pediatric acute-onset neuropsychiatric syndrome (PANS):  
948 recommendations from the 2013 PANS Consensus Conference. *J Child Adolesc*  
949 *Psychopharmacol* 2015 Feb;25(1):3-13.
- 950 (18) Chan A, Gao J, Houston M, Willett T, Farhadian B, Silverman M, et al. Children With PANS  
951 May Manifest POTS. *Front Neurol* 2022 Apr 26;13:819636.
- 952 (19) Fernandez F, Soon I, Li Z, Kuan TC, Min DH, Wong ES, et al. Wip1 phosphatase positively  
953 modulates dendritic spine morphology and memory processes through the p38MAPK signaling  
954 pathway. *Cell Adh Migr* 2012;6(4):333-343.
- 955 (20) Tang Y, Pan B, Zhou X, Xiong K, Gao Q, Huang L, et al. Wip1-dependent modulation of  
956 macrophage migration and phagocytosis. *Redox Biol* 2017 Oct;13:665-673.
- 957 (21) Brichkina A, Bulavin DV. WIP-ing out atherosclerosis with autophagy. *Autophagy* 2012  
958 Oct;8(10):1545-1547.
- 959 (22) Sun B, Hu X, Liu G, Ma B, Xu Y, Yang T, et al. Phosphatase Wip1 negatively regulates  
960 neutrophil migration and inflammation. *J Immunol* 2014 Feb 1;192(3):1184-1195.

- 961 (23) Barnes J, Salas F, Mokhtari R, Dolstra H, Pedrosa E, Lachman HM. Modeling the  
962 neuropsychiatric manifestations of Lowe syndrome using induced pluripotent stem cells:  
963 defective F-actin polymerization and WAVE-1 expression in neuronal cells. *Mol Autism* 2018  
964 Aug 15;9:44-3. eCollection 2018.
- 965 (24) Olivier E, Qiu C, Bouhassira EE. Novel, high-yield red blood cell production methods from  
966 CD34-positive cells derived from human embryonic stem, yolk sac, fetal liver, cord blood, and  
967 peripheral blood. *Stem Cells Transl Med* 2012 Aug;1(8):604-614.
- 968 (25) Ran FA, Hsu PD, Lin CY, Gootenberg JS, Konermann S, Trevino AE, et al. Double nicking  
969 by RNA-guided CRISPR Cas9 for enhanced genome editing specificity. *Cell* 2013 Sep  
970 12;154(6):1380-1389.
- 971 (26) Zhang Y, Pak C, Han Y, Ahlenius H, Zhang Z, Chanda S, et al. Rapid single-step induction  
972 of functional neurons from human pluripotent stem cells. *Neuron* 2013 Jun 5;78(5):785-798.
- 973 (27) Meijering E, Jacob M, Sarria JC, Steiner P, Hirling H, Unser M. Design and validation of a  
974 tool for neurite tracing and analysis in fluorescence microscopy images. *Cytometry A* 2004  
975 Apr;58(2):167-176.
- 976 (28) Kulej K, Avgousti DC, Sidoli S, Herrmann C, Della Fera AN, Kim ET, et al. Time-resolved  
977 Global and Chromatin Proteomics during Herpes Simplex Virus Type 1 (HSV-1) Infection. *Mol*  
978 *Cell Proteomics* 2017 Apr;16(4 suppl 1):S92-S107.
- 979 (29) Aguilan JT, Kulej K, Sidoli S. Guide for protein fold change and p-value calculation for non-  
980 experts in proteomics. *Mol Omics* 2020 Dec 1;16(6):573-582.
- 981 (30) Engholm-Keller K, Birck P, Størling J, Pociot F, Mandrup-Poulsen T, Larsen MR. TiSH--a  
982 robust and sensitive global phosphoproteomics strategy employing a combination of TiO<sub>2</sub>,  
983 SIMAC, and HILIC. *J Proteomics* 2012 Oct 22;75(18):5749-5761.
- 984 (31) Thingholm TE, Larsen MR. The Use of Titanium Dioxide for Selective Enrichment of  
985 Phosphorylated Peptides. *Methods Mol Biol* 2016;1355:135-146.
- 986 (32) Eden E, Navon R, Steinfeld I, Lipson D, Yakhini Z. GOrilla: a tool for discovery and  
987 visualization of enriched GO terms in ranked gene lists. *BMC Bioinformatics* 2009 Feb 3;10:48-  
988 48.
- 989 (33) Chou MF, Schwartz D. Biological sequence motif discovery using motif-x. *Curr Protoc*  
990 *Bioinformatics* 2011 Sep;Chapter 13:Unit 13.15-24.
- 991 (34) Song C, Ye M, Liu Z, Cheng H, Jiang X, Han G, et al. Systematic analysis of protein  
992 phosphorylation networks from phosphoproteomic data. *Mol Cell Proteomics* 2012  
993 Oct;11(10):1070-1083.
- 994 (35) Raaijmakers LM, Giansanti P, Possik PA, Mueller J, Peeper DS, Heck AJ, et al.  
995 PhosphoPath: Visualization of Phosphosite-centric Dynamics in Temporal Molecular Networks.  
996 *J Proteome Res* 2015 Oct 2;14(10):4332-4341.

- 997 (36) Wilk AJ, Rustagi A, Zhao NQ, Roque J, Martinez-Colon GJ, McKechnie JL, et al. A single-  
998 cell atlas of the peripheral immune response to severe COVID-19. medRxiv 2020 Apr 23.
- 999 (37) Wang P, Su H, Zhang L, Chen H, Hu X, Yang F, et al. Phosphatase wild-type p53-induced  
1000 phosphatase 1 controls the development of T(H)9 cells and allergic airway inflammation. J  
1001 Allergy Clin Immunol 2018 Jun;141(6):2168-2181.
- 1002 (38) Schito ML, Demidov ON, Saito S, Ashwell JD, Appella E. Wip1 phosphatase-deficient mice  
1003 exhibit defective T cell maturation due to sustained p53 activation. J Immunol 2006 Apr  
1004 15;176(8):4818-4825.
- 1005 (39) Challakkara MF, Chhabra R. snoRNAs in hematopoiesis and blood malignancies: A  
1006 comprehensive review. J Cell Physiol 2023 Jun;238(6):1207-1225.
- 1007 (40) Dar AA, Sawada K, Dybas JM, Moser EK, Lewis EL, Park E, et al. The E3 ubiquitin ligase  
1008 Cul4b promotes CD4+ T cell expansion by aiding the repair of damaged DNA. PLoS Biol 2021  
1009 Feb 1;19(2):e3001041.
- 1010 (41) Li T, Wu S, Jia L, Cao W, Yao Y, Zhao G, et al. CUL4 E3 ligase regulates the proliferation  
1011 and apoptosis of lung squamous cell carcinoma and small cell lung carcinoma. Cancer Biol Med  
1012 2020 May 15;17(2):357-370.
- 1013 (42) Liu H, Lu W, He H, Wu J, Zhang C, Gong H, et al. Inflammation-dependent overexpression  
1014 of c-Myc enhances CRL4(DCAF4) E3 ligase activity and promotes ubiquitination of ST7 in  
1015 colitis-associated cancer. J Pathol 2019 Aug;248(4):464-475.
- 1016 (43) Lopes F, Torres F, Soares G, Barbosa M, Silva J, Duque F, et al. Genomic imbalances  
1017 defining novel intellectual disability associated loci. Orphanet J Rare Dis 2019 Jul 5;14(1):164-0.
- 1018 (44) Guan J, Liu X, Zhang H, Lv Y, Wang X, Yang X, et al. Generation of an iPSC line  
1019 (SDQLChi015-A) from peripheral blood mononuclear cells of a patient with mental retardation  
1020 type 15 carrying c.1007\_1011del, p.(Ile336fs) in CUL4B gene. Stem Cell Res 2019  
1021 Dec;41:101628.
- 1022 (45) Kampmeier A, Leitão E, Parenti I, Beygo J, Depienne C, Bramswig NC, et al. PHIP-  
1023 associated Chung-Jansen syndrome: Report of 23 new individuals. Front Cell Dev Biol 2023  
1024 Jan 16;10:1020609.
- 1025 (46) López M, Pérez-Grijalba V, García-Cobaleda I, Domínguez-Garrido E. A 22.5 kb deletion in  
1026 CUL4B causing Cabezas syndrome identified using CNV approach from WES data. Clin Case  
1027 Rep 2020 Sep 29;8(12):3184-3188.
- 1028 (47) Song Y, Li P, Qin L, Xu Z, Jiang B, Ma C, et al. CUL4B negatively regulates Toll-like  
1029 receptor-triggered proinflammatory responses by repressing Pten transcription. Cell Mol  
1030 Immunol 2021 Feb;18(2):339-349.
- 1031 (48) Xu Z, Li L, Qian Y, Song Y, Qin L, Duan Y, et al. Upregulation of IL-6 in CUL4B-deficient  
1032 myeloid-derived suppressive cells increases the aggressiveness of cancer cells. Oncogene  
1033 2019 Jul;38(30):5860-5872.

- 1034 (49) Zhao Z, Wang H, Kang N, Wang Z, Hou X, Hu L, et al. Aurora kinase a promotes the  
1035 progression of papillary thyroid carcinoma by activating the mTORC2-AKT signalling pathway.  
1036 *Cell Biosci* 2022 Dec 5;12(1):195-z.
- 1037 (50) Chiuso F, Delle Donne R, Giamundo G, Rinaldi L, Borzacchiello D, Moraca F, et al.  
1038 Ubiquitylation of BBSome is required for ciliary assembly and signaling. *EMBO Rep* 2023 Feb  
1039 6:e55571.
- 1040 (51) Kattan RE, Han H, Seo G, Yang B, Lin Y, Dotson M, et al. Interactome Analysis of Human  
1041 Phospholipase D and Phosphatidic Acid-Associated Protein Network. *Mol Cell Proteomics* 2022  
1042 Feb;21(2):100195.
- 1043 (52) Smith CE, Tsai YC, Liang Y, Khago D, Mariano J, Li J, et al. A structurally conserved site in  
1044 AUP1 binds the E2 enzyme UBE2G2 and is essential for ER-associated degradation. *PLoS Biol*  
1045 2021 Dec 8;19(12):e3001474.
- 1046 (53) Cristea I, Bruland O, Rødahl E, Bredrup C. K(+) regulates relocation of Pellino-2 to the site  
1047 of NLRP3 inflammasome activation in macrophages. *FEBS Lett* 2021 Oct;595(19):2437-2446.
- 1048 (54) Bögershausen N, Wollnik B. Mutational Landscapes and Phenotypic Spectrum of  
1049 SWI/SNF-Related Intellectual Disability Disorders. *Front Mol Neurosci* 2018 Aug 3;11:252.
- 1050 (55) Sun X, Cheng L, Sun Y. Autism-associated protein POGZ controls ESCs and ESC neural  
1051 induction by association with esBAF. *Mol Autism* 2022 Jun 1;13(1):24-9.
- 1052 (56) Shillington A, Pedapati E, Hopkin R, Suhrie K. Early behavioral and developmental  
1053 interventions in ADNP-syndrome: A case report of SWI/SNF-related neurodevelopmental  
1054 syndrome. *Mol Genet Genomic Med* 2020 Jun;8(6):e1230.
- 1055 (57) D'Incal CP, Van Rossem KE, De Man K, Konings A, Van Dijck A, Rizzuti L, et al. Chromatin  
1056 remodeler Activity-Dependent Neuroprotective Protein (ADNP) contributes to syndromic autism.  
1057 *Clin Epigenetics* 2023 Mar 21;15(1):45-8.
- 1058 (58) O'Leary PC, Chen H, Doruk YU, Williamson T, Polacco B, McNeal AS, et al. Resistance to  
1059 ATR Inhibitors Is Mediated by Loss of the Nonsense-Mediated Decay Factor UPF2. *Cancer Res*  
1060 2022 Nov 2;82(21):3950-3961.
- 1061 (59) Johnson JL, Stoica L, Liu Y, Zhu PJ, Bhattacharya A, Buffington SA, et al. Inhibition of  
1062 Upf2-Dependent Nonsense-Mediated Decay Leads to Behavioral and Neurophysiological  
1063 Abnormalities by Activating the Immune Response. *Neuron* 2019 Nov 20;104(4):665-679.e8.
- 1064 (60) James MO, Jahn SC, Zhong G, Smeltz MG, Hu Z, Stacpoole PW. Therapeutic applications  
1065 of dichloroacetate and the role of glutathione transferase zeta-1. *Pharmacol Ther* 2017  
1066 Feb;170:166-180.
- 1067 (61) Gao Q, Cheng B, Chen C, Lei C, Lin X, Nie D, et al. Dysregulated glucuronic acid  
1068 metabolism exacerbates hepatocellular carcinoma progression and metastasis through the  
1069 TGF $\beta$  signalling pathway. *Clin Transl Med* 2022 Aug;12(8):e995.

- 1070 (62) Aborode AT, Pustake M, Awuah WA, Alwerdani M, Shah P, Yarlagadda R, et al. Targeting  
1071 Oxidative Stress Mechanisms to Treat Alzheimer's and Parkinson's Disease: A Critical Review.  
1072 *Oxid Med Cell Longev* 2022 Jul 31;2022:7934442.
- 1073 (63) Alqahtani T, Deore SL, Kide AA, Shende BA, Sharma R, Chakole RD, et al. Mitochondrial  
1074 dysfunction and oxidative stress in Alzheimer's disease, and Parkinson's disease, Huntington's  
1075 disease and Amyotrophic Lateral Sclerosis -An updated review. *Mitochondrion* 2023 Jun 1.
- 1076 (64) Jiménez-Vacas JM, Herrero-Aguayo V, Montero-Hidalgo AJ, Gómez-Gómez E, Fuentes-  
1077 Fayos AC, León-González AJ, et al. Dysregulation of the splicing machinery is directly  
1078 associated to aggressiveness of prostate cancer. *EBioMedicine* 2020 Jan;51:102547.
- 1079 (65) Song X, Ma J. SRRM1 promotes the proliferation, migration, and invasion of hepatocellular  
1080 carcinoma cells by regulating the JAK/STAT signaling pathway. *Tissue Cell* 2022  
1081 Dec;79:101954.
- 1082 (66) Østvold AC, Grundt K, Wiese C. NUCKS1 is a highly modified, chromatin-associated  
1083 protein involved in a diverse set of biological and pathophysiological processes. *Biochem J*  
1084 2022 Jun 17;479(11):1205-1220.
- 1085 (67) Maranon DG, Sharma N, Huang Y, Selemenakis P, Wang M, Altina N, et al. NUCKS1  
1086 promotes RAD54 activity in homologous recombination DNA repair. *J Cell Biol* 2020 Oct  
1087 5;219(10):e201911049. doi: 10.1083/jcb.201911049.
- 1088 (68) Yue Y, Leung SG, Liu Y, Huang Y, Grundt K, Østvold A, et al. Nucks1 synergizes with  
1089 Trp53 to promote radiation lymphomagenesis in mice. *Oncotarget* 2016 Sep 20;7(38):61874-  
1090 61889.
- 1091 (69) Pan H, Liu Z, Ma J, Li Y, Zhao Y, Zhou X, et al. Genome-wide association study using  
1092 whole-genome sequencing identifies risk loci for Parkinson's disease in Chinese population.  
1093 *NPJ Parkinsons Dis* 2023 Feb 9;9(1):22-6.
- 1094 (70) Yamaguchi H, Durell SR, Chatterjee DK, Anderson CW, Appella E. The Wip1 phosphatase  
1095 PPM1D dephosphorylates SQ/TQ motifs in checkpoint substrates phosphorylated by PI3K-like  
1096 kinases. *Biochemistry* 2007 Nov 6;46(44):12594-12603.
- 1097 (71) Hehr U, Uyanik G, Aigner L, Couillard-Despres S, Winkler J. DCX-Related Disorders. In:  
1098 Adam MP, Ardinger HH, Pagon RA, Wallace SE, Bean LJH, Stephens K, et al, editors.  
1099 *GeneReviews*(®) Seattle (WA): University of Washington, Seattle. GeneReviews is a registered  
1100 trademark of the University of Washington, Seattle; 1993.
- 1101 (72) Hughes HK, R J Moreno, Ashwood P. Innate immune dysfunction and neuroinflammation in  
1102 autism spectrum disorder (ASD). *Brain Behav Immun* 2023 Feb;108:245-254.
- 1103 (73) Lampiasi N, Bonaventura R, Deidda I, Zito F, Russo R. Inflammation and the Potential  
1104 Implication of Macrophage-Microglia Polarization in Human ASD: An Overview. *Int J Mol Sci*  
1105 2023 Jan 31;24(3):2703. doi: 10.3390/ijms24032703.

- 1106 (74) Zhao D, Mokhtari R, Pedrosa E, Birnbaum R, Zheng D, Lachman HM. Transcriptome  
1107 analysis of microglia in a mouse model of Rett syndrome: differential expression of genes  
1108 associated with microglia/macrophage activation and cellular stress. *Mol Autism* 2017 Mar  
1109 29;8:17-z. eCollection 2017.
- 1110 (75) Derecki NC, Cronk JC, Lu Z, Xu E, Abbott SB, Guyenet PG, et al. Wild-type microglia  
1111 arrest pathology in a mouse model of Rett syndrome. *Nature* 2012 Apr 5;484(7392):105-109.
- 1112 (76) Verma N, Velmurugan GV, Winford E, Coburn H, Kotiya D, Leibold N, et al. A $\beta$  efflux  
1113 impairment and inflammation linked to cerebrovascular accumulation of amyloid-forming amylin  
1114 secreted from pancreas. *Commun Biol* 2023 Jan 3;6(1):2-2.
- 1115 (77) Martinez-Lozada Z, Robinson MB. Reciprocal communication between astrocytes and  
1116 endothelial cells is required for astrocytic glutamate transporter 1 (GLT-1) expression.  
1117 *Neurochem Int* 2020 Oct;139:104787.
- 1118 (78) Zhen H, Zhao L, Ling Z, Kuo L, Xue X, Feng J. Wip1 regulates blood-brain barrier function  
1119 and neuro-inflammation induced by lipopolysaccharide via the sonic hedgehog signaling  
1120 signaling pathway. *Mol Immunol* 2018 Jan;93:31-37.
- 1121 (79) Olcum M, Tastan B, Kiser C, Genc S, Genc K. Microglial NLRP3 inflammasome activation  
1122 in multiple sclerosis. *Adv Protein Chem Struct Biol* 2020;119:247-308.
- 1123 (80) Anderson FL, Biggs KE, Rankin BE, Havrda MC. NLRP3 inflammasome in  
1124 neurodegenerative disease. *Transl Res* 2022 Aug 8.
- 1125 (81) Braatz C, Komes MP, Ravichandran KA, de Fragas MG, Griep A, Schwartz S, et al.  
1126 NLRP3-directed antisense oligonucleotides reduce microglial immunoactivities in vitro. *J*  
1127 *Neurochem* 2023 Feb 17.
- 1128 (82) Deng Z, Zhou X, Lu J, Yue Z. Autophagy deficiency in neurodevelopmental disorders. *Cell*  
1129 *Biosci* 2021 Dec 17;11(1):214-x.
- 1130 (83) Zhang Q, Sterling K, Xu L, Xing M, Cai F, Yu S, et al. CNTNAP2 Protein Is Degraded by  
1131 the Ubiquitin-Proteasome System and the Macroautophagy-Lysosome Pathway. *Mol Neurobiol*  
1132 2023 May;60(5):2455-2469.
- 1133 (84) Zapata-Muñoz J, Villarejo-Zori B, Largo-Barrientos P, Boya P. Towards a better  
1134 understanding of the neuro-developmental role of autophagy in sickness and in health. *Cell*  
1135 *Stress* 2021 Jun 29;5(7):99-118.
- 1136 (85) Choi I, Heaton GR, Lee YK, Yue Z. Regulation of  $\alpha$ -synuclein homeostasis and  
1137 inflammasome activation by microglial autophagy. *Sci Adv* 2022 Oct 28;8(43):eabn1298.
- 1138 (86) Lv N, Zhao Y, Liu X, Ye L, Liang Z, Kang Y, et al. Dysfunctional telomeres through  
1139 mitostress-induced cGAS/STING activation to aggravate immune senescence and viral  
1140 pneumonia. *Aging Cell* 2022 Apr;21(4):e13594.

- 1141 (87) Harper JW, Schulman BA. Cullin-RING Ubiquitin Ligase Regulatory Circuits: A Quarter  
1142 Century Beyond the F-Box Hypothesis. *Annu Rev Biochem* 2021 Jun 20;90:403-429.
- 1143 (88) Hill S, Reichermeier K, Scott DC, Samentar L, Coulombe-Huntington J, Izzi L, et al. Robust  
1144 cullin-RING ligase function is established by a multiplicity of poly-ubiquitylation pathways. *Elife*  
1145 2019 Dec 23;8:10.7554/eLife.51163.
- 1146 (89) Gan Z, Wang B, Lu Y, Cai S, Cai J, Jian J, et al. Molecular characterization and expression  
1147 of CD2BP2 in Nile tilapia (*Oreochromis niloticus*) in response to *Streptococcus agalactiae*  
1148 stimulus. *Gene* 2014 Sep 10;548(1):126-133.
- 1149 (90) Blasi G, Bortoletto E, Gasparotto M, Filippini F, Bai C, Rosani U, et al. A glimpse on  
1150 metazoan ZNFX1 helicases, ancient players of antiviral innate immunity. *Fish Shellfish Immunol*  
1151 2022 Feb;121:456-466.
- 1152 (91) Zhang L, Ko C, Li Y, Jie Z, Zhu L, Zhou X, et al. Peli1 facilitates NLRP3 inflammasome  
1153 activation by mediating ASC ubiquitination. *Cell Rep* 2021 Oct 26;37(4):109904.
- 1154 (92) Xu J, Yu T, Pietronigro EC, Yuan J, Arioli J, Pei Y, et al. Peli1 impairs microglial A $\beta$   
1155 phagocytosis through promoting C/EBP $\beta$  degradation. *PLoS Biol* 2020 Oct 5;18(10):e3000837.
- 1156 (93) Zhou W, Wang J, Wang X, Wang B, Zhao Z, Fu J, et al. Degradation of HDAC10 by  
1157 autophagy promotes IRF3-mediated antiviral innate immune responses. *Sci Signal* 2022 Dec  
1158 20;15(765):eabo4356.
- 1159 (94) Pan M, Yin Y, Hu T, Wang X, Jia T, Sun J, et al. UXT attenuates the CGAS-STING1  
1160 signaling by targeting STING1 for autophagic degradation. *Autophagy* 2023 Feb;19(2):440-456.
- 1161 (95) Oduro PK, Zheng X, Wei J, Yang Y, Wang Y, Zhang H, et al. The cGAS-STING signaling in  
1162 cardiovascular and metabolic diseases: Future novel target option for pharmacotherapy. *Acta*  
1163 *Pharm Sin B* 2022 Jan;12(1):50-75.
- 1164 (96) Al Hamrashdi M, Brady G. Regulation of IRF3 activation in human antiviral signaling  
1165 pathways. *Biochem Pharmacol* 2022 Jun;200:115026.
- 1166 (97) Stupfler B, Verriez C, Gallois-Montbrun S, Marquet R, Paillart J. Degradation-Independent  
1167 Inhibition of APOBEC3G by the HIV-1 Vif Protein. *Viruses* 2021 Apr 3;13(4):617. doi:  
1168 10.3390/v13040617.
- 1169 (98) Bao Q, Zhou J. Various strategies for developing APOBEC3G protectors to circumvent  
1170 human immunodeficiency virus type 1. *Eur J Med Chem* 2023 Feb 6;250:115188.
- 1171 (99) Sharma S, Wang J, Alqassim E, Portwood S, Cortes Gomez E, Maguire O, et al.  
1172 Mitochondrial hypoxic stress induces widespread RNA editing by APOBEC3G in natural killer  
1173 cells. *Genome Biol* 2019 Feb 21;20(1):37-1.
- 1174 (100) Salter JD, Polevoda B, Bennett RP, Smith HC. Regulation of Antiviral Innate Immunity  
1175 Through APOBEC Ribonucleoprotein Complexes. *Subcell Biochem* 2019;93:193-219.

- 1176 (101) Yuan Y, Qin H, Li H, Shi W, Bao L, Xu S, et al. The Functional Roles of ISG15/ISGylation  
1177 in Cancer. *Molecules* 2023 Jan 31;28(3):1337. doi: 10.3390/molecules28031337.
- 1178 (102) Papparisto E, Woods MW, Coleman MD, Moghadasi SA, Kochar DS, Tom SK, et al.  
1179 Evolution-Guided Structural and Functional Analyses of the HERC Family Reveal an Ancient  
1180 Marine Origin and Determinants of Antiviral Activity. *J Virol* 2018 Jun 13;92(13):e00528-18. Print  
1181 2018 Jul 1.
- 1182 (103) Jacquet S, Pontier D, Etienne L. Rapid Evolution of HERC6 and Duplication of a Chimeric  
1183 HERC5/6 Gene in Rodents and Bats Suggest an Overlooked Role of HERCs in Mammalian  
1184 Immunity. *Front Immunol* 2020 Dec 18;11:605270.
- 1185 (104) Heath J, Cheyou ES, Findlay S, Luo VM, Carpio EP, Lee J, et al. POGZ promotes  
1186 homology-directed DNA repair in an HP1-dependent manner. *EMBO Rep* 2022 Jan  
1187 5;23(1):e51041.
- 1188 (105) Conrow-Graham M, Williams JB, Martin J, Zhong P, Cao Q, Rein B, et al. A convergent  
1189 mechanism of high risk factors ADNP and POGZ in neurodevelopmental disorders. *Brain* 2022  
1190 Sep 14;145(9):3250-3263.
- 1191 (106) Bruno LP, Doddato G, Valentino F, Baldassarri M, Tita R, Fallerini C, et al. New  
1192 Candidates for Autism/Intellectual Disability Identified by Whole-Exome Sequencing. *Int J Mol*  
1193 *Sci* 2021 Dec 14;22(24):13439. doi: 10.3390/ijms222413439.
- 1194 (107) Merriweather A, Murdock DR, Rosenfeld JA, Dai H, Ketkar S, Emrick L, et al. A novel, de  
1195 novo intronic variant in POGZ causes White-Sutton syndrome. *Am J Med Genet A* 2022  
1196 Jul;188(7):2198-2203.
- 1197 (108) Markenscoff-Papadimitriou E, Binyameen F, Whalen S, Price J, Lim K, Ypsilanti AR, et al.  
1198 Autism risk gene POGZ promotes chromatin accessibility and expression of clustered synaptic  
1199 genes. *Cell Rep* 2021 Dec 7;37(10):110089.
- 1200 (109) Tammimies K. Genetic mechanisms of regression in autism spectrum disorder. *Neurosci*  
1201 *Biobehav Rev* 2019 Jul;102:208-220.
- 1202 (110) Van Dijck A, Vandeweyer G, Kooy F. ADNP-Related Disorder. In: Adam MP, Mirzaa GM,  
1203 Pagon RA, Wallace SE, Bean LJH, Gripp KW, et al, editors. *GeneReviews*(®) Seattle (WA):  
1204 University of Washington, Seattle. *GeneReviews* is a registered trademark of the University of  
1205 Washington, Seattle. All rights reserved; 1993.
- 1206 (111) Ganaiem M, Karmon G, Ivashko-Pachima Y, Gozes I. Distinct Impairments Characterizing  
1207 Different ADNP Mutants Reveal Aberrant Cytoplasmic-Nuclear Crosstalk. *Cells* 2022 Sep  
1208 26;11(19):2994. doi: 10.3390/cells11192994.
- 1209 (112) Bellon M, Nicot C. Feedback Loop Regulation between Pim Kinases and Tax Keeps  
1210 Human T-Cell Leukemia Virus Type 1 Viral Replication in Check. *J Virol* 2022 Feb  
1211 9;96(3):e0196021-21. Epub 2021 Nov 24.

- 1212 (113) Clements AN, Warfel NA. Targeting PIM Kinases to Improve the Efficacy of  
1213 Immunotherapy. *Cells* 2022 Nov 21;11(22):3700. doi: 10.3390/cells11223700.
- 1214 (114) van der Graaf A, Zorro MM, Claringbould A, Vösa U, Aguirre-Gamboa R, Li C, et al.  
1215 Systematic Prioritization of Candidate Genes in Disease Loci Identifies TRAFD1 as a Master  
1216 Regulator of IFN $\gamma$  Signaling in Celiac Disease. *Front Genet* 2021 Jan 25;11:562434.
- 1217 (115) Sanada T, Takaesu G, Mashima R, Yoshida R, Kobayashi T, Yoshimura A. FLN29  
1218 deficiency reveals its negative regulatory role in the Toll-like receptor (TLR) and retinoic acid-  
1219 inducible gene I (RIG-I)-like helicase signaling pathway. *J Biol Chem* 2008 Dec  
1220 5;283(49):33858-33864.
- 1221 (116) Cleverley K, Lee WC, Mumford P, Collins T, Rickman M, Cunningham TJ, et al. A novel  
1222 knockout mouse for the small EDRK-rich factor 2 (Serf2) showing developmental and other  
1223 deficits. *Mamm Genome* 2021 Apr;32(2):94-103.
- 1224 (117) Chen B, Sheng D, Wang C, Liu W, Hu A, Xiao X, et al. FLI1 regulates inflammation-  
1225 associated genes to accelerate leukemogenesis. *Cell Signal* 2022 Apr;92:110269.
- 1226 (118) Jiang Q, Wang Y, Xiang M, Hua J, Zhou T, Chen F, et al. UFL1, a UFMylation E3 ligase,  
1227 plays a crucial role in multiple cellular stress responses. *Front Endocrinol (Lausanne)* 2023 Feb  
1228 10;14:1123124.
- 1229 (119) Li J, Tang X, Tu X, Jin Z, Dong H, Yang Q, et al. UFL1 alleviates ER stress and apoptosis  
1230 stimulated by LPS via blocking the ferroptosis pathway in human granulosa-like cells. *Cell*  
1231 *Stress Chaperones* 2022 Sep;27(5):485-497.
- 1232 (120) Fang Z, Pan Z. Essential Role of Ubiquitin-Fold Modifier 1 Conjugation in DNA Damage  
1233 Response. *DNA Cell Biol* 2019 Oct;38(10):1030-1039.
- 1234 (121) Wang Y, Que H, Rong Y. Autophagosomal components recycling on autolysosomes.  
1235 *Trends Cell Biol* 2022 Nov;32(11):897-899.
- 1236 (122) Shi Z, Chen S, Han X, Peng R, Luo J, Yang L, et al. The rare mutation in the endosome-  
1237 associated recycling protein gene VPS50 is associated with human neural tube defects. *Mol*  
1238 *Cytogenet* 2019 Feb 20;12:8-9. eCollection 2019.
- 1239 (123) Majerczyk D, Ayad EG, Brewton KL, Saing P, Hart PC. Systemic maternal inflammation  
1240 promotes ASD via IL-6 and IFN- $\gamma$ . *Biosci Rep* 2022 Nov 30;42(11):BSR20220713. doi:  
1241 10.1042/BSR20220713.
- 1242 (124) Ma Y, Wang J, Guo S, Meng Z, Ren Y, Xie Y, et al. Cytokine/chemokine levels in the CSF  
1243 and serum of anti-NMDAR encephalitis: A systematic review and meta-analysis. *Front Immunol*  
1244 2023 Jan 23;13:1064007.
- 1245 (125) Mousten IV, Sørensen NV, Christensen RHB, Benros ME. Cerebrospinal Fluid  
1246 Biomarkers in Patients With Unipolar Depression Compared With Healthy Control Individuals: A  
1247 Systematic Review and Meta-analysis. *JAMA Psychiatry* 2022 Jun 1;79(6):571-581.

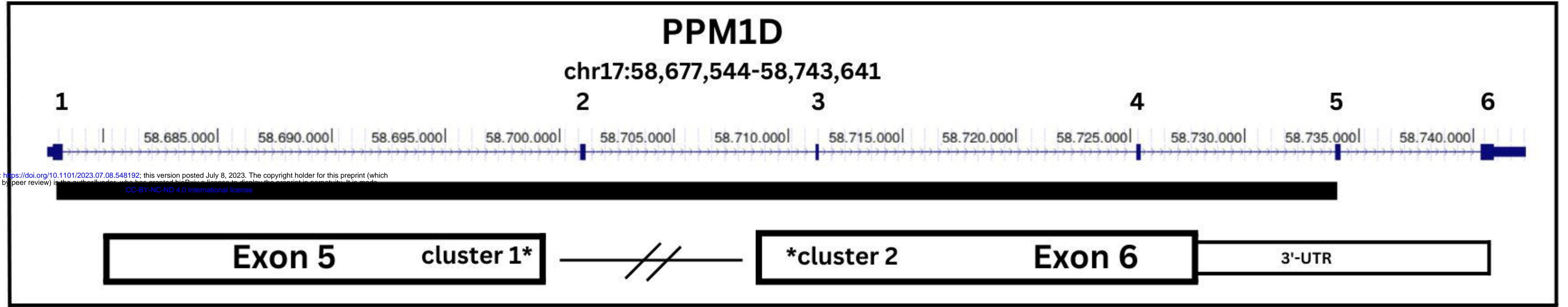
- 1248 (126) Kwon J, Suessmilch M, McColl A, Cavanagh J, Morris BJ. Distinct trans-placental effects  
1249 of maternal immune activation by TLR3 and TLR7 agonists: implications for schizophrenia risk.  
1250 Sci Rep 2021 Dec 13;11(1):23841-9.
- 1251 (127) Poli A, Abdul-Hamid S, Zaurito AE, Campagnoli F, Bevilacqua V, Sheth B, et al. PIP4Ks  
1252 impact on PI3K, FOXP3, and UHRF1 signaling and modulate human regulatory T cell  
1253 proliferation and immunosuppressive activity. Proc Natl Acad Sci U S A 2021 Aug  
1254 3;118(31):e2010053118. doi: 10.1073/pnas.2010053118.
- 1255 (128) Wu J, Wang M, Chen H, Xu J, Zhang G, Gu C, et al. The Rare Variant rs35356162 in  
1256 UHRF1BP1 Increases Bladder Cancer Risk in Han Chinese Population. Front Oncol 2020 Feb  
1257 11;10:134.
- 1258 (129) Grünblatt E, Oneda B, Ekici AB, Ball J, Geissler J, Uebe S, et al. High resolution  
1259 chromosomal microarray analysis in paediatric obsessive-compulsive disorder. BMC Med  
1260 Genomics 2017 Nov 28;10(1):68-5.
- 1261 (130) Granek Z, Barczuk J, Siwecka N, Rozpędek-Kamińska W, Kucharska E, Majsterek I.  
1262 GBA1 Gene Mutations in  $\alpha$ -Synucleinopathies-Molecular Mechanisms Underlying Pathology  
1263 and Their Clinical Significance. Int J Mol Sci 2023 Jan 20;24(3):2044. doi:  
1264 10.3390/ijms24032044.
- 1265 (131) Parlar SC, Grenn FP, Kim JJ, Baluwendraat C, Gan-Or Z. Classification of GBA1 Variants  
1266 in Parkinson's Disease: The GBA1-PD Browser. Mov Disord 2023 Jan 4.
- 1267 (132) Vitner EB, Farfel-Becker T, Ferreira NS, Leshkowitz D, Sharma P, Lang KS, et al.  
1268 Induction of the type I interferon response in neurological forms of Gaucher disease. J  
1269 Neuroinflammation 2016 May 12;13(1):104-2.
- 1270 (133) Liu Q, Shen Z, Pan H, Ma S, Xiong F, He F. The molecular mechanism of Gaucher  
1271 disease caused by compound heterozygous mutations in GBA1 gene. Front Pediatr 2023 Jan  
1272 26;11:1092645.
- 1273 (134) Xu Y, Li Y, Wang C, Han T, Liu H, Sun L, et al. The reciprocal interactions between  
1274 microglia and T cells in Parkinson's disease: a double-edged sword. J Neuroinflammation 2023  
1275 Feb 12;20(1):33-y.
- 1276 (135) Nair-Gupta P, Baccarini A, Tung N, Seyffer F, Florey O, Huang Y, et al. TLR signals  
1277 induce phagosomal MHC-I delivery from the endosomal recycling compartment to allow cross-  
1278 presentation. Cell 2014 Jul 31;158(3):506-521.
- 1279 (136) Heo AJ, Kim SB, Ji CH, Han D, Lee SJ, Lee SH, et al. The N-terminal cysteine is a dual  
1280 sensor of oxygen and oxidative stress. Proc Natl Acad Sci U S A 2021 Dec  
1281 14;118(50):e2107993118. doi: 10.1073/pnas.2107993118.
- 1282 (137) Tripathi S, Pohl MO, Zhou Y, Rodriguez-Frandsen A, Wang G, Stein DA, et al. Meta- and  
1283 Orthogonal Integration of Influenza "OMICs" Data Defines a Role for UBR4 in Virus Budding.  
1284 Cell Host Microbe 2015 Dec 9;18(6):723-735.

- 1285 (138) Morrison J, Laurent-Rolle M, Maestre AM, Rajsbaum R, Pisanelli G, Simon V, et al.  
1286 Dengue virus co-opts UBR4 to degrade STAT2 and antagonize type I interferon signaling. *PLoS*  
1287 *Pathog* 2013 Mar;9(3):e1003265.
- 1288 (139) Cavallieri F, Cury RG, Guimarães T, Fioravanti V, Grisanti S, Rossi J, et al. Recent  
1289 Advances in the Treatment of Genetic Forms of Parkinson's Disease: Hype or Hope? *Cells*  
1290 2023 Feb 27;12(5):764. doi: 10.3390/cells12050764.
- 1291 (140) Jia F, Fellner A, Kumar KR. Monogenic Parkinson's Disease: Genotype, Phenotype,  
1292 Pathophysiology, and Genetic Testing. *Genes (Basel)* 2022 Mar 7;13(3):471. doi:  
1293 10.3390/genes13030471.
- 1294 (141) Bayón Y, Trinidad AG, de la Puerta ML, Del Carmen Rodríguez M, Bogetz J, Rojas A, et  
1295 al. KCTD5, a putative substrate adaptor for cullin3 ubiquitin ligases. *FEBS J* 2008  
1296 Aug;275(15):3900-3910.
- 1297 (142) Young BD, Sha J, Vashisht AA, Wohlschlegel JA. Human Multisubunit E3 Ubiquitin Ligase  
1298 Required for Heterotrimeric G-Protein  $\beta$ -Subunit Ubiquitination and Downstream Signaling. *J*  
1299 *Proteome Res* 2021 Sep 3;20(9):4318-4330.
- 1300 (143) Chang MY, Kang I, Gale MJ, Manicone AM, Kinsella MG, Braun KR, et al. Versican is  
1301 produced by Trif- and type I interferon-dependent signaling in macrophages and contributes to  
1302 fine control of innate immunity in lungs. *Am J Physiol Lung Cell Mol Physiol* 2017 Dec  
1303 1;313(6):L1069-L1086.
- 1304 (144) Boeing S, Williamson L, Encheva V, Gori I, Saunders RE, Instrell R, et al. Multiomic  
1305 Analysis of the UV-Induced DNA Damage Response. *Cell Rep* 2016 May 17;15(7):1597-1610.
- 1306 (145) Uesaka N, Uchigashima M, Mikuni T, Hirai H, Watanabe M, Kano M. Retrograde signaling  
1307 for climbing fiber synapse elimination. *Cerebellum* 2015 Feb;14(1):4-7.
- 1308 (146) Hridi SU, Barbour M, Wilson C, Franssen AJ, Harte T, Bushell TJ, et al. Increased Levels  
1309 of IL-16 in the Central Nervous System during Neuroinflammation Are Associated with  
1310 Infiltrating Immune Cells and Resident Glial Cells. *Biology (Basel)* 2021 May 27;10(6):472. doi:  
1311 10.3390/biology10060472.
- 1312 (147) Kouchaki E, Akbari H, Mahmoudi F, Salehi M, Naimi E, Nikoueinejad H. Correlation of  
1313 Serum Levels of Interleukine-16, CCL27, Tumor Necrosis Factor-related Apoptosis-inducing  
1314 Ligand, and B-cell Activating Factor with Multiple Sclerosis Severity. *Iran J Allergy Asthma*  
1315 *Immunol* 2022 Feb 6;21(1):27-34.
- 1316 (148) Saito S, Cao D, Victor AR, Peng Z, Wu H, Okwan-Duodu D. RASAL3 Is a Putative  
1317 RasGAP Modulating Inflammatory Response by Neutrophils. *Front Immunol* 2021 Oct  
1318 27;12:744300.
- 1319 (149) Wang J, Wang G, Cheng D, Huang S, Chang A, Tan X, et al. Her2 promotes early  
1320 dissemination of breast cancer by suppressing the p38-MK2-Hsp27 pathway that is targetable  
1321 by Wip1 inhibition. *Oncogene* 2020 Oct;39(40):6313-6326.

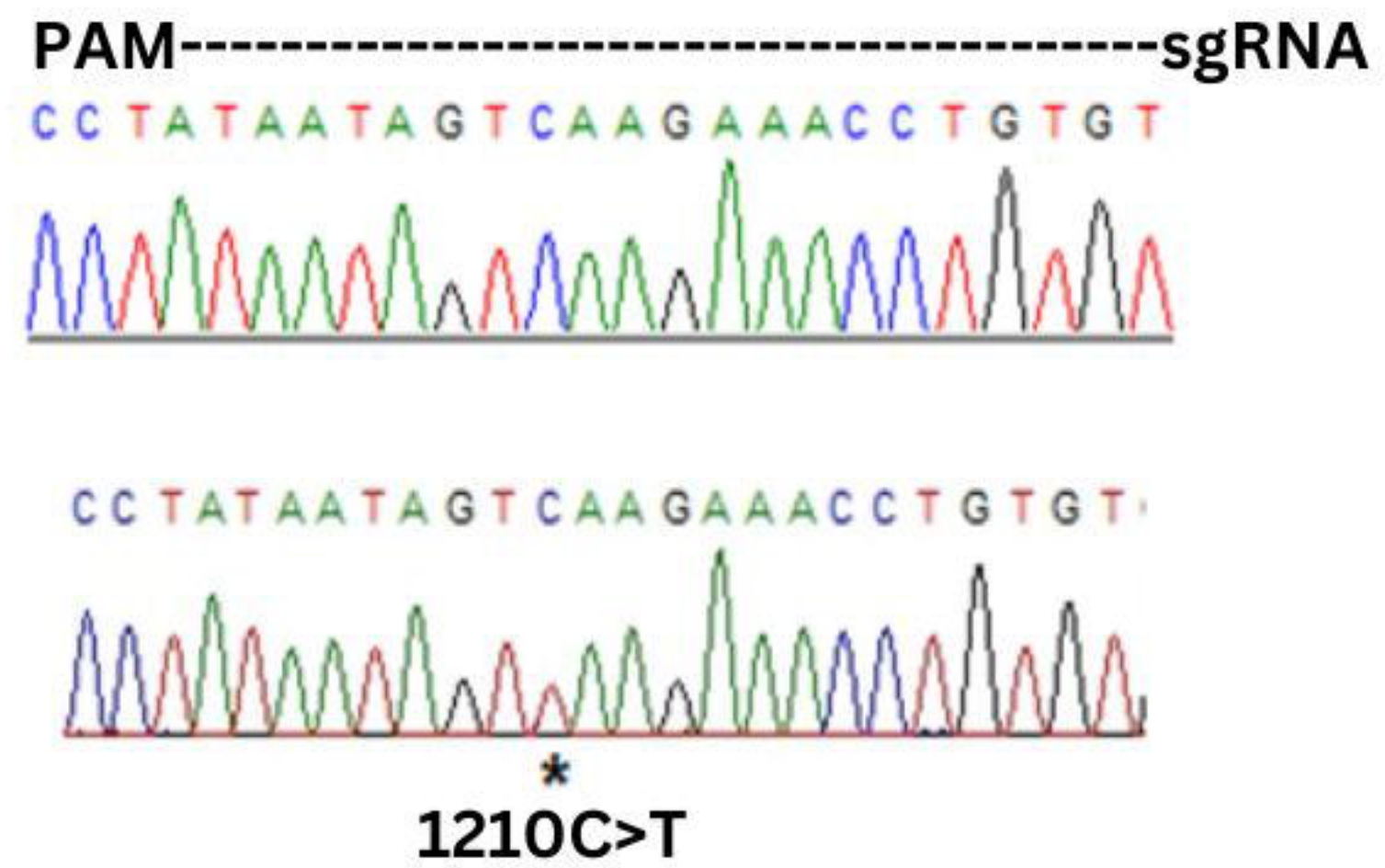
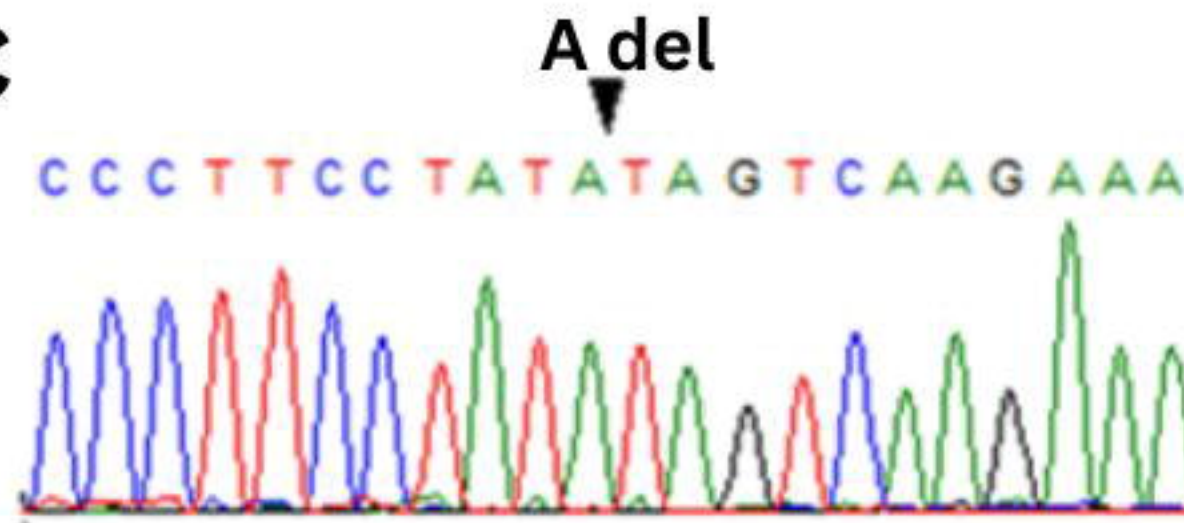
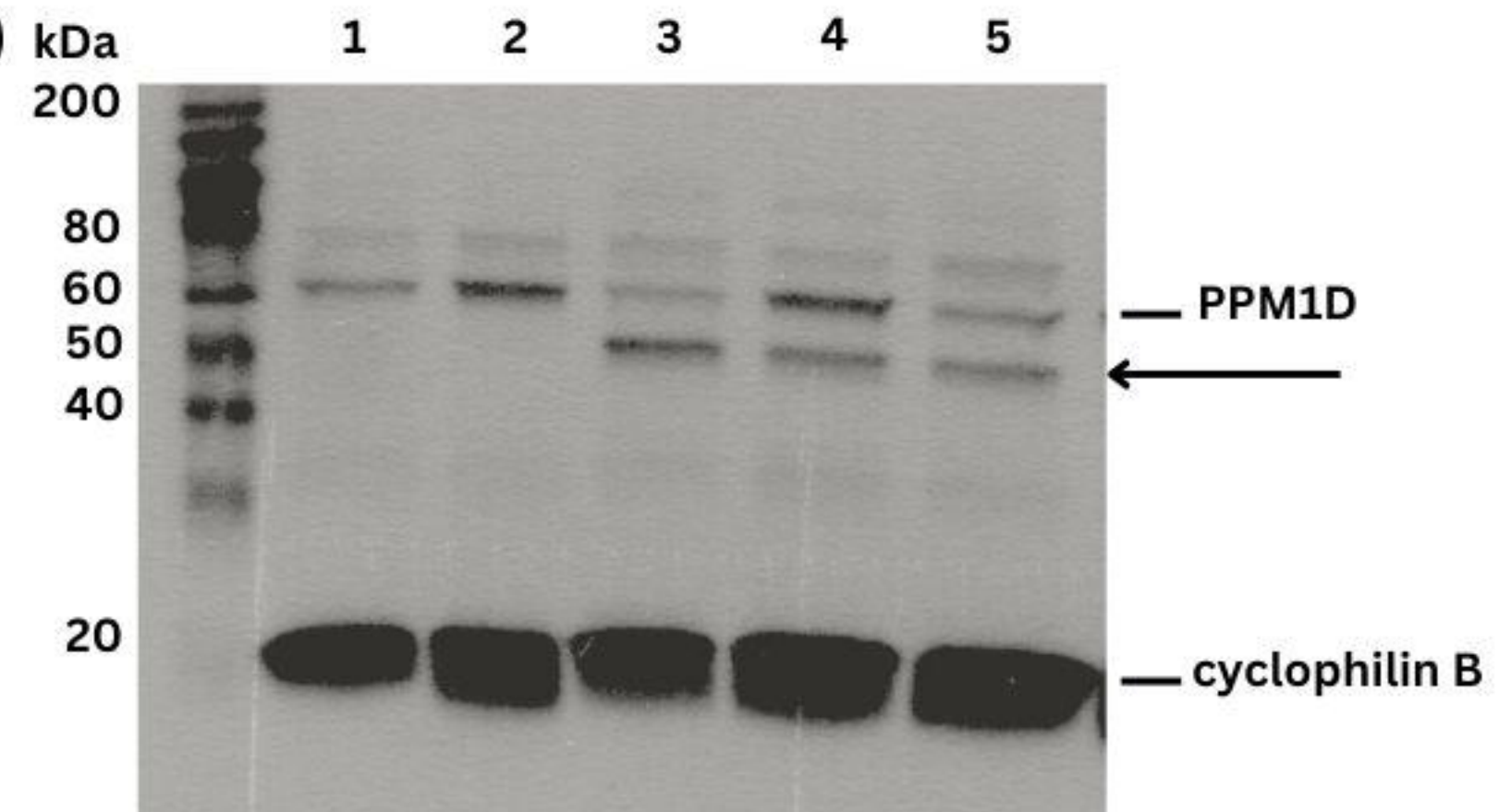
- 1322 (150) Demidov ON, Kek C, Shreeram S, Timofeev O, Fornace AJ, Appella E, et al. The role of  
1323 the MKK6/p38 MAPK pathway in Wip1-dependent regulation of ErbB2-driven mammary gland  
1324 tumorigenesis. *Oncogene* 2007 Apr 12;26(17):2502-2506.
- 1325 (151) Ledonne A, Mercuri NB. On the Modulatory Roles of Neuregulins/ErbB Signaling on  
1326 Synaptic Plasticity. *Int J Mol Sci* 2019 Dec 31;21(1):275. doi: 10.3390/ijms21010275.
- 1327 (152) Spahic H, Parmar P, Miller S, Emerson PC, Lechner C, St Pierre M, et al. Dysregulation of  
1328 ErbB4 Signaling Pathway in the Dorsal Hippocampus after Neonatal Hypoxia-Ischemia and Late  
1329 Deficits in PV(+) Interneurons, Synaptic Plasticity and Working Memory. *Int J Mol Sci* 2022 Dec  
1330 28;24(1):508. doi: 10.3390/ijms24010508.
- 1331 (153) Chen Y, Hu N, Wu D, Bi L, Luo Z, Huang L, et al. PV network plasticity mediated by  
1332 neuregulin1-ErbB4 signalling controls fear extinction. *Mol Psychiatry* 2022 Feb;27(2):896-906.
- 1333 (154) Shi L, Bergson CM. Neuregulin 1: an intriguing therapeutic target for neurodevelopmental  
1334 disorders. *Transl Psychiatry* 2020 Jun 16;10(1):190-5.
- 1335 (155) Meldolesi J. Post-Synapses in the Brain: Role of Dendritic and Spine Structures.  
1336 *Biomedicines* 2022 Aug 2;10(8):1859. doi: 10.3390/biomedicines10081859.
- 1337 (156) Hori K, Shimaoka K, Hoshino M. AUTS2 Gene: Keys to Understanding the Pathogenesis  
1338 of Neurodevelopmental Disorders. *Cells* 2021 Dec 21;11(1):11. doi: 10.3390/cells11010011.
- 1339 (157) DeGiosio RA, Grubisha MJ, MacDonald ML, McKinney BC, Camacho CJ, Sweet RA.  
1340 More than a marker: potential pathogenic functions of MAP2. *Front Mol Neurosci* 2022 Sep  
1341 16;15:974890.
- 1342 (158) Goodwill AM, Low LT, Fox PT, Fox PM, Poon KK, Bhowmick SS, et al. Meta-analytic  
1343 connectivity modelling of functional magnetic resonance imaging studies in autism spectrum  
1344 disorders. *Brain Imaging Behav* 2023 Jan 12.
- 1345 (159) Fabozzi F, Margoni S, Andreozzi B, Musci MS, Del Baldo G, Boccuto L, et al. Cerebellar  
1346 mutism syndrome: From pathophysiology to rehabilitation. *Front Cell Dev Biol* 2022 Dec  
1347 2;10:1082947.
- 1348 (160) Pang EW, Hammill C, Taylor MJ, Near J, Schachar R, Crosbie J, et al. Cerebellar  
1349 gamma-aminobutyric acid: Investigation of group effects in neurodevelopmental disorders.  
1350 *Autism Res* 2023 Mar;16(3):535-542.
- 1351 (161) Whiteley P, Marlow B, Kapoor RR, Blagojevic-Stokic N, Sala R. Autoimmune Encephalitis  
1352 and Autism Spectrum Disorder. *Front Psychiatry* 2021 Dec 17;12:775017.
- 1353 (162) Malek M, Ashraf-Ganjouei A, Moradi K, Bagheri S, Mohammadi M, Akhondzadeh S.  
1354 Prednisolone as Adjunctive Treatment to Risperidone in Children With Regressive Type of  
1355 Autism Spectrum Disorder: A Randomized, Placebo-Controlled Trial. *Clin Neuropharmacol*  
1356 2020;43(2):39-45.

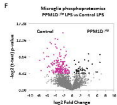
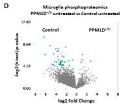
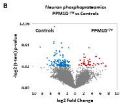
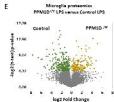
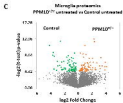
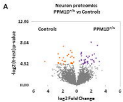
- 1357 (163) Harutyunyan AA, Harutyunyan HA, Yenkeyan KB. Novel Probable Glimpse at Inflammatory  
1358 Scenario Development in Autistic Pathology. *Front Psychiatry* 2021 Dec 22;12:788779.
- 1359 (164) Santoro JD, Partridge R, Tanna R, Pagarkar D, Khoshnood M, Rehmani M, et al.  
1360 Evidence of neuroinflammation and immunotherapy responsiveness in individuals with down  
1361 syndrome regression disorder. *J Neurodev Disord* 2022 Jun 3;14(1):35-w.
- 1362 (165) Golla S, Sweeney JA. Corticosteroid therapy in regressive autism: Preliminary findings  
1363 from a retrospective study. *BMC Med* 2014 May 15;12:79-79.
- 1364 (166) Bey AL, Gorman MP, Gallentine W, Kohlenberg TM, Frankovich J, Jiang YH, et al.  
1365 Subacute Neuropsychiatric Syndrome in Girls With SHANK3 Mutations Responds to  
1366 Immunomodulation. *Pediatrics* 2020 Feb;145(2):e20191490. doi: 10.1542/peds.2019-1490.
- 1367 (167) Ferguson BJ, Marler S, Altstein LL, Lee EB, Mazurek MO, McLaughlin A, et al.  
1368 Associations between cytokines, endocrine stress response, and gastrointestinal symptoms in  
1369 autism spectrum disorder. *Brain Behav Immun* 2016 Nov;58:57-62.
- 1370 (168) Lee R, Funk KE. Imaging blood-brain barrier disruption in neuroinflammation and  
1371 Alzheimer's disease. *Front Aging Neurosci* 2023 Mar 17;15:1144036.
- 1372 (169) Park JS, Choe K, Khan A, Jo MH, Park HY, Kang MH, et al. Establishing Co-Culture  
1373 Blood-Brain Barrier Models for Different Neurodegeneration Conditions to Understand Its Effect  
1374 on BBB Integrity. *Int J Mol Sci* 2023 Mar 9;24(6):5283. doi: 10.3390/ijms24065283.
- 1375 (170) Jasiak-Zatońska M, Pietrzak A, Wyciszkiwicz A, Więsik-Szewczyk E, Pawlak-Buś K,  
1376 Leszczyński P, et al. Different blood-brain-barrier disruption profiles in multiple sclerosis,  
1377 neuromyelitis optica spectrum disorders, and neuropsychiatric systemic lupus erythematosus.  
1378 *Neurol Neurochir Pol* 2022;56(3):246-255.
- 1379 (171) Ju J, Su Y, Zhou Y, Wei H, Xu Q. The SARS-CoV-2 envelope protein disrupts barrier  
1380 function in an in vitro human blood-brain barrier model. *Front Cell Neurosci* 2022 Aug  
1381 23;16:897564.
- 1382 (172) Yamano K, Youle RJ. PINK1 is degraded through the N-end rule pathway. *Autophagy*  
1383 2013 Nov 1;9(11):1758-1769.
- 1384 (173) Olagunju AS, Ahammad F, Alagbe AA, Otenaike TA, Teibo JO, Mohammad F, et al.  
1385 Mitochondrial dysfunction: A notable contributor to the progression of Alzheimer's and  
1386 Parkinson's disease. *Heliyon* 2023 Mar 11;9(3):e14387.
- 1387 (174) Han R, Liu Y, Li S, Li X, Yang W. PINK1-PRKN mediated mitophagy: differences between  
1388 in vitro and in vivo models. *Autophagy* 2023 May;19(5):1396-1405.
- 1389 (175) Monies D, Abouelhoda M, AlSayed M, Alhassnan Z, Alotaibi M, Kayyali H, et al. The  
1390 landscape of genetic diseases in Saudi Arabia based on the first 1000 diagnostic panels and  
1391 exomes. *Hum Genet* 2017 Aug;136(8):921-939.

- 1392 (176) Yang J, Ran M, Li H, Lin Y, Ma K, Yang Y, et al. New insight into neurological  
1393 degeneration: Inflammatory cytokines and blood-brain barrier. *Front Mol Neurosci* 2022 Oct  
1394 24;15:1013933.
- 1395 (177) Soltani Khaboushan A, Pahlevan-Fallahy M, Shobeiri P, Teixeira AL, Rezaei N. Cytokines  
1396 and chemokines profile in encephalitis patients: A meta-analysis. *PLoS One* 2022 Sep  
1397 1;17(9):e0273920.
- 1398 (178) Kunz N, Kemper C. Complement Has Brains-Do Intracellular Complement and  
1399 Immunometabolism Cooperate in Tissue Homeostasis and Behavior? *Front Immunol* 2021 Feb  
1400 25;12:629986.
- 1401 (179) Dodd WS, Patel D, Lucke-Wold B, Hosaka K, Chalouhi N, Hoh BL. Adropin decreases  
1402 endothelial monolayer permeability after cell-free hemoglobin exposure and reduces MCP-1-  
1403 induced macrophage transmigration. *Biochem Biophys Res Commun* 2021 Dec 10;582:105-  
1404 110.
- 1405 (180) Tammimies K. Genetic mechanisms of regression in autism spectrum disorder. *Neurosci*  
1406 *Biobehav Rev* 2019 Jul;102:208-220.
- 1407
- 1408

**A**

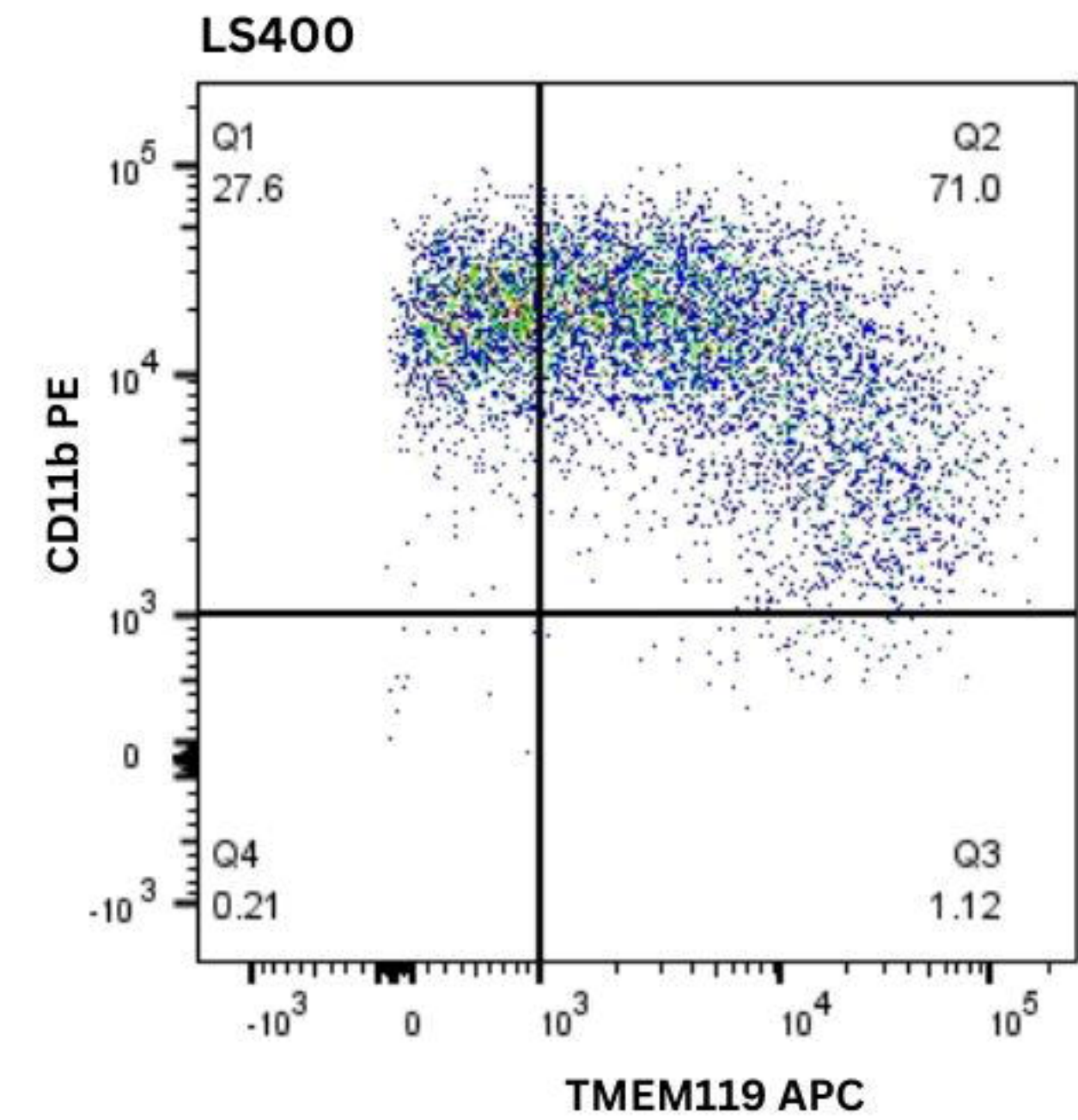
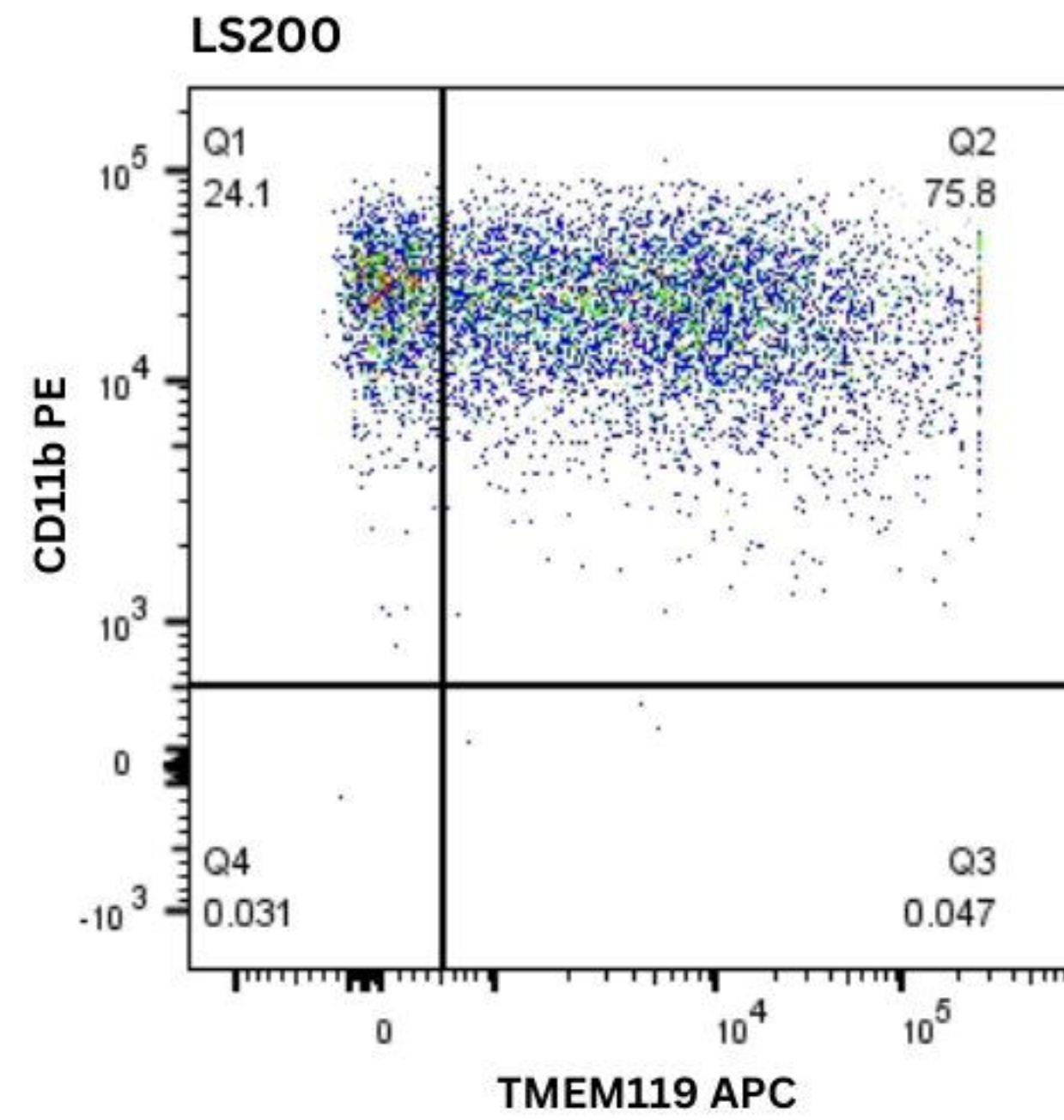
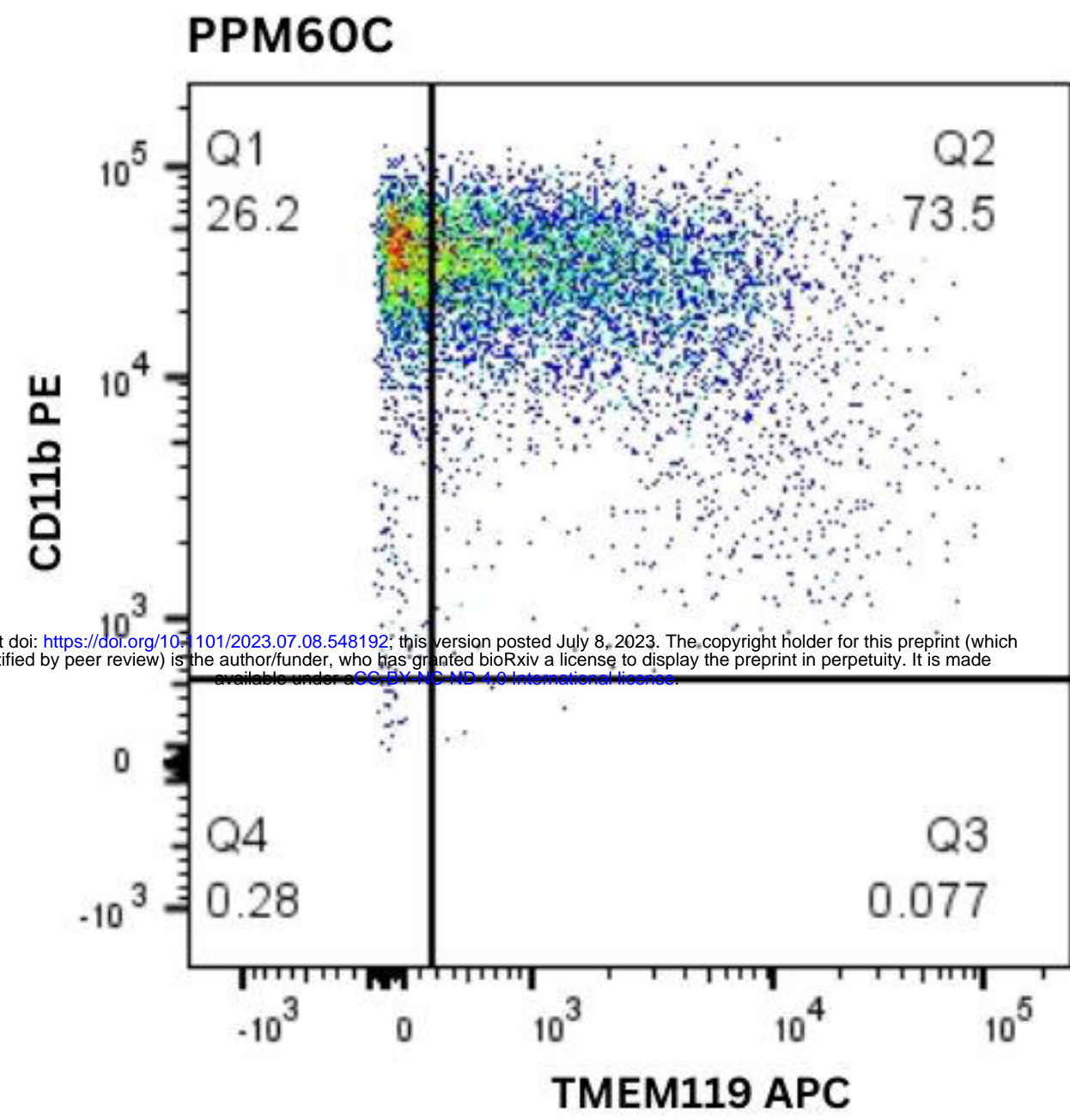
bioRxiv preprint doi: <https://doi.org/10.1101/2023.07.08.548192>; this version posted July 8, 2023. The copyright holder for this preprint (which was not certified by peer review) is the author/funder, who has granted bioRxiv a license to display the preprint in perpetuity. It is made available under aCC-BY-NC-ND 4.0 International license.

**B****C****D**



Control

bioRxiv preprint doi: <https://doi.org/10.1101/2023.07.08.548192>; this version posted July 8, 2023. The copyright holder for this preprint (which was not certified by peer review) is the author/funder, who has granted bioRxiv a license to display the preprint in perpetuity. It is made available under aCC-BY-NC-ND 4.0 International license.



PPM1D<sup>+/tr</sup>

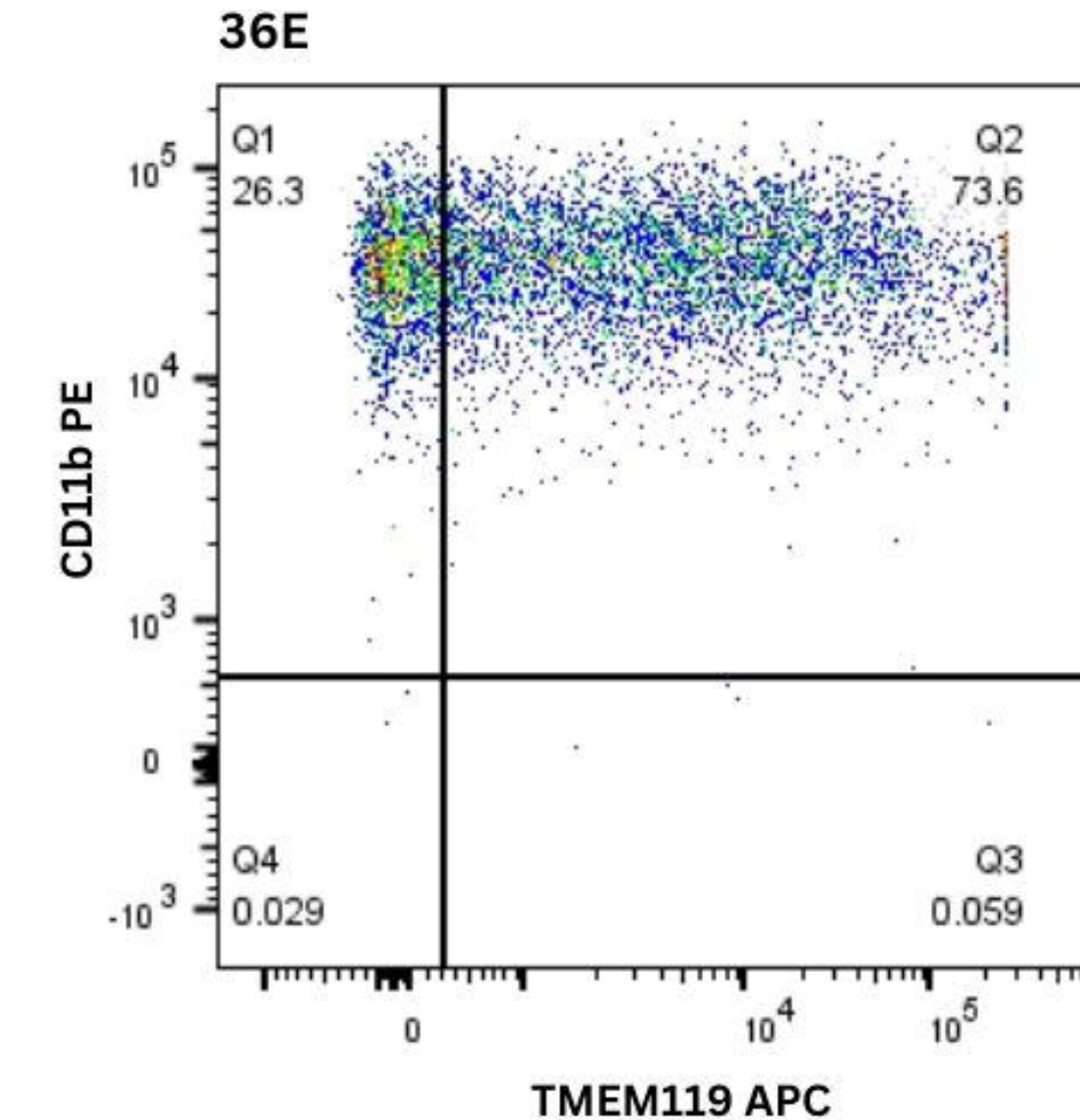
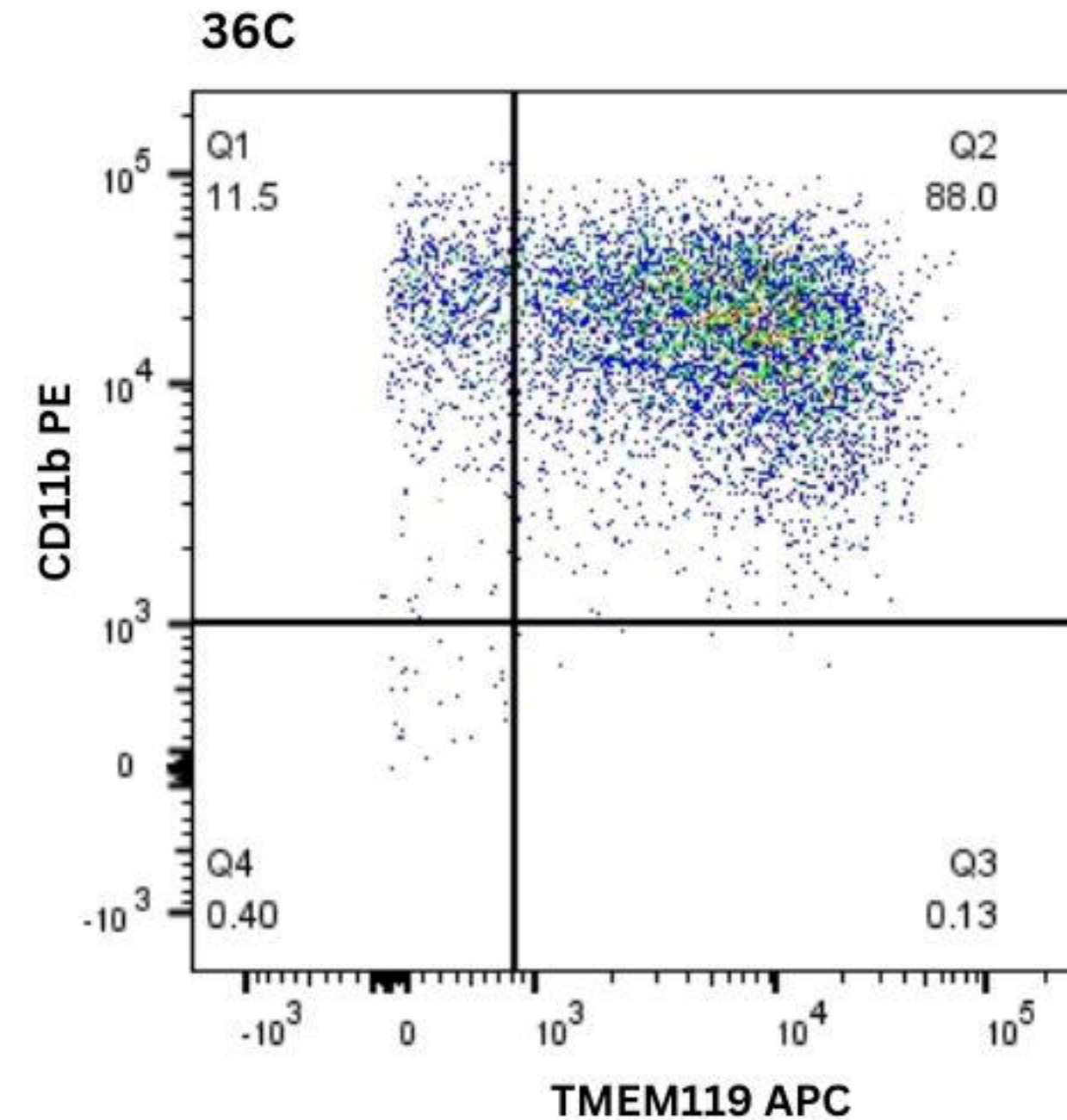
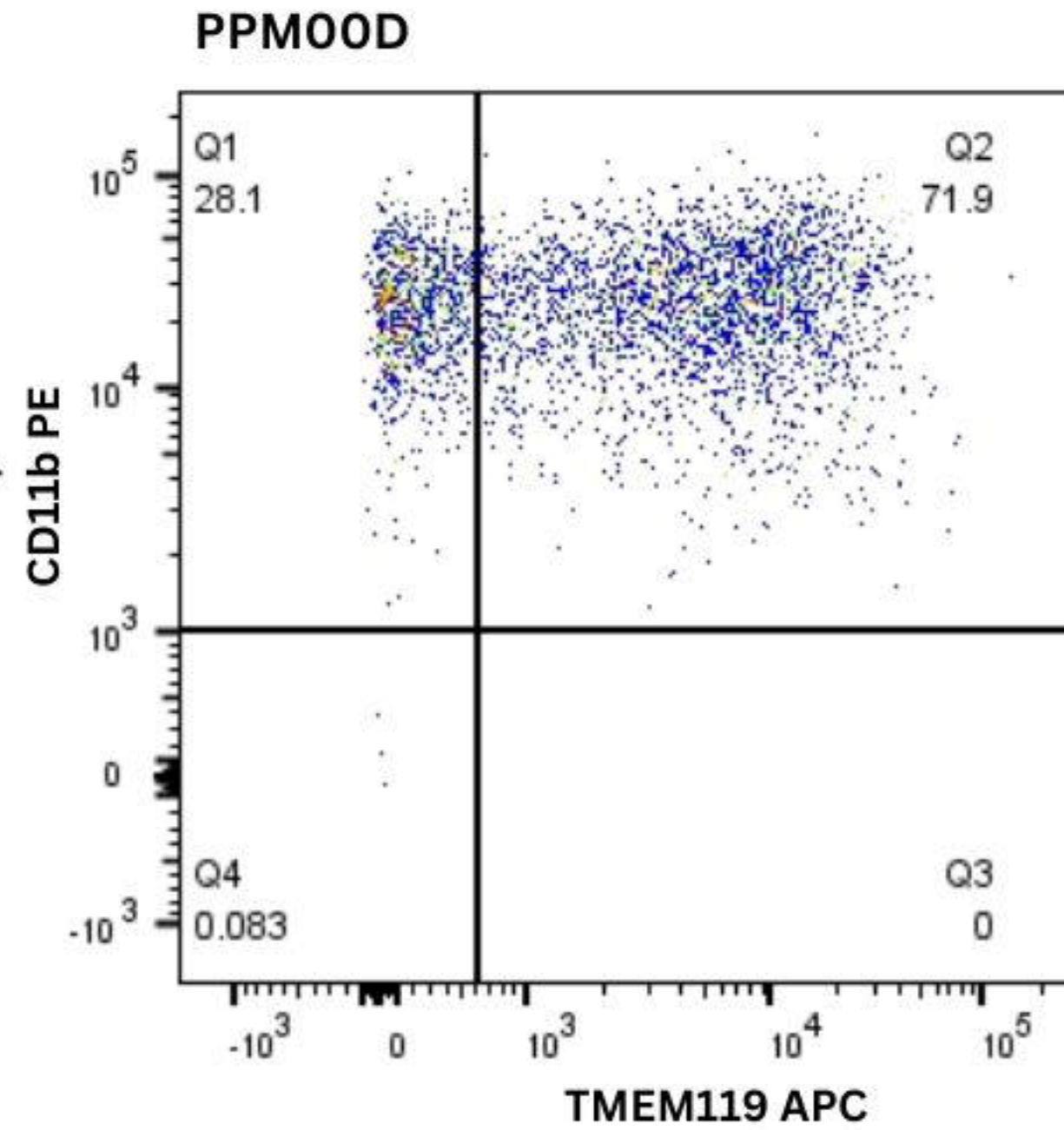
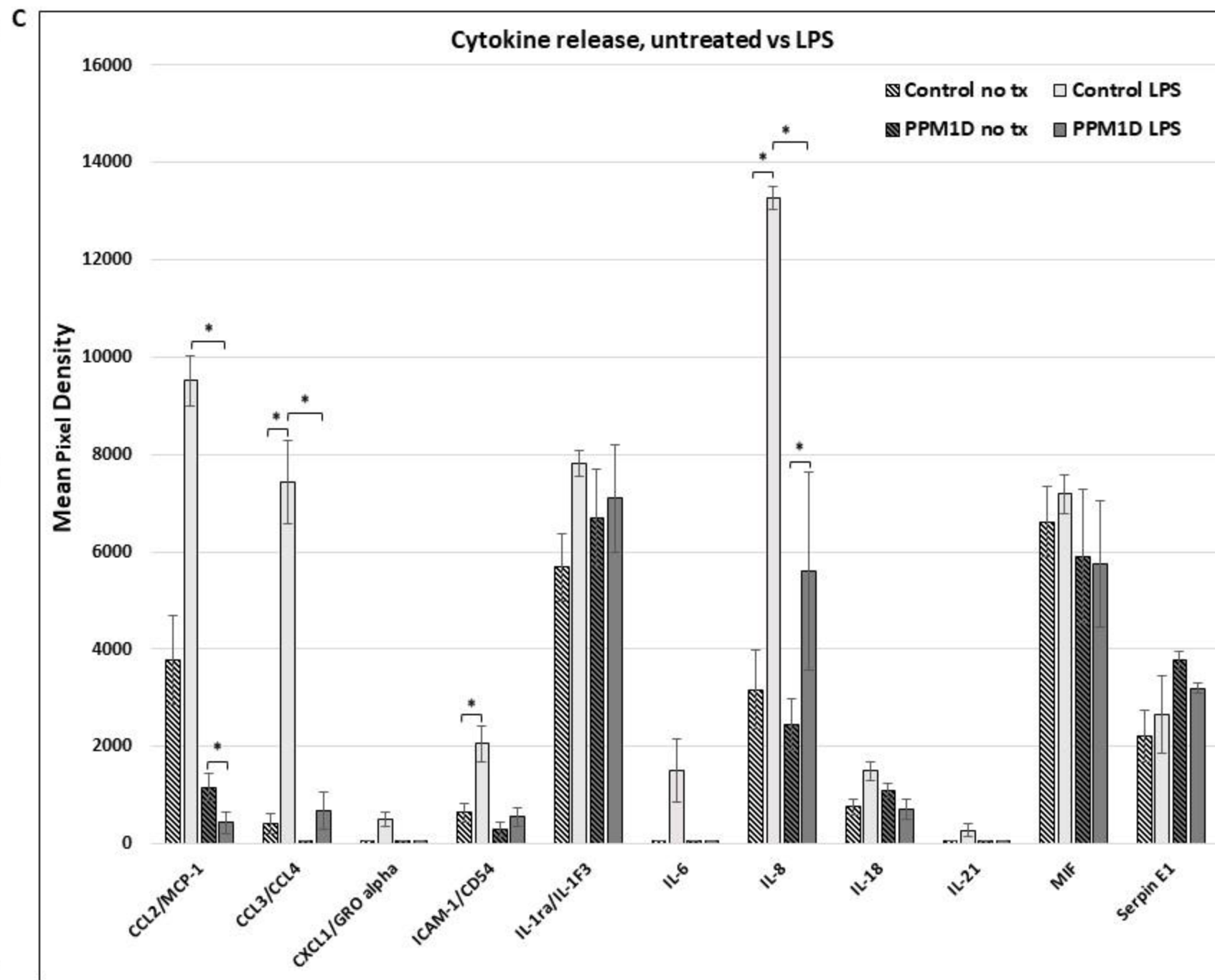
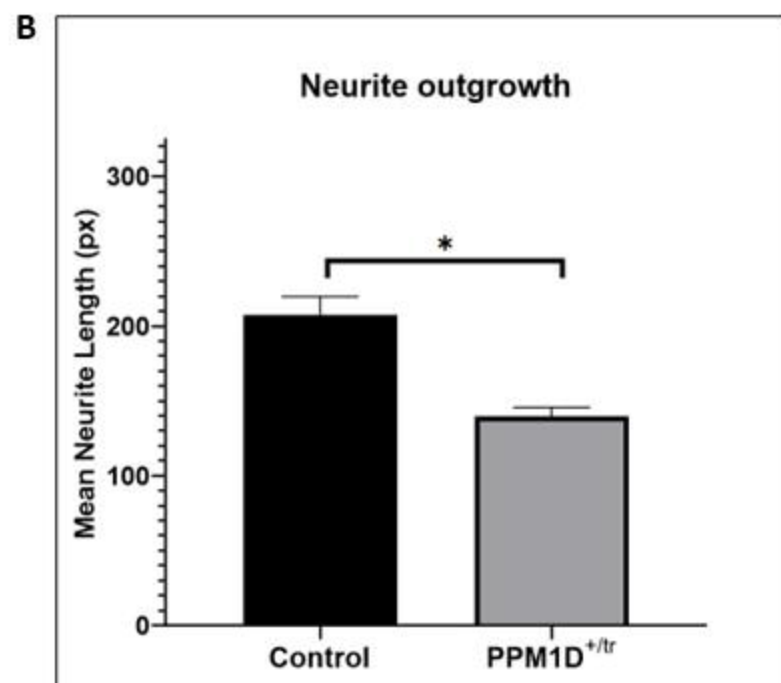
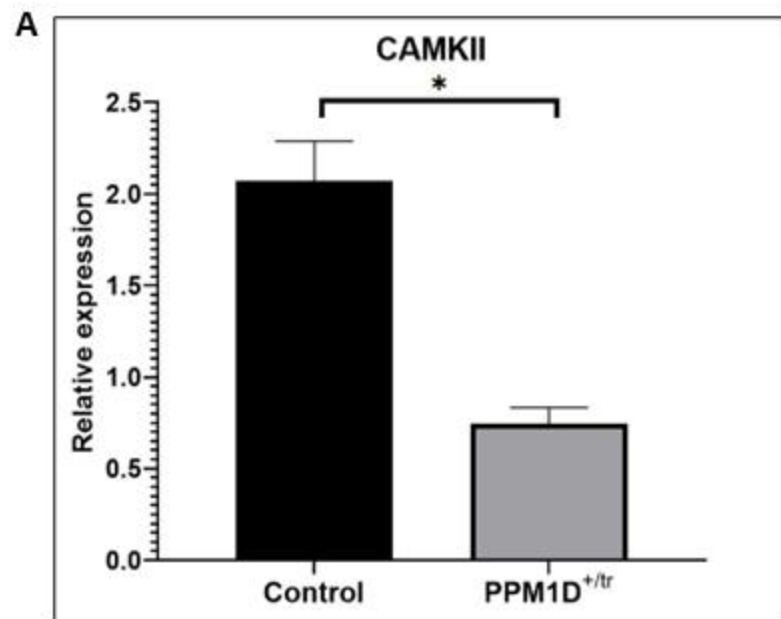


Figure 4

<b>Summary of neuronal and microglia proteomics and phosphoproteomics</b>						
<b>GO or KEGG Pathways</b>	<b>Neuron proteomics</b>	<b>Nueron phospho prote omics</b>	<b>Microglia prote omics</b>	<b>Microglia phospho proteomics</b>	<b>LPS Microglica prote omics</b>	<b>LPS microglia phospho proteomics</b>
<b>Ubiquitin ligase/ regulators</b>	shared	shared	shared	shared	shared	shared
<b>Chromatin</b>	shared	shared	shared	shared	not shared	shared
<b>Splicing/spliceosome</b>	shared	shared	not shared	shared	shared	shared
<b>Cytoskeleton</b>	not shared	shared	not shared	shared	not shared	shared
<b>ErbB Signaling</b>	shared	shared	shared	shared	shared	shared
<b>Neurodegenerative Disorder</b>	shared	not shared	shared	not shared	shared	not shared

■ shared

■ not shared



<b>GO term</b>	<b>Neuron Proteomics: Biological Processes</b>	<b>P-value</b>
GO:0045582	positive regulation of T cell differentiation	7.36E-06
GO:0000495	box H/ACA snoRNA 3'-end processing	1.30E-05
GO:0034964	box H/ACA snoRNA processing	1.30E-05
GO:0000375	RNA splicing, via transesterification reactions	2.09E-05
GO:0031126	snoRNA 3'-end processing	2.31E-05
GO:0006397	mRNA processing	2.77E-05
GO:0000377	RNA splicing, via transesterification with bulged adenosine as nucleophile	3.12E-05
GO:0000398	mRNA splicing, via spliceosome	3.12E-05
GO:0043144	snoRNA processing	3.33E-05
GO:0033979	box H/ACA snoRNA metabolic process	3.81E-05
GO:0090669	telomerase RNA stabilization	3.81E-05
GO:0045580	regulation of T cell differentiation	8.72E-05
GO:0045621	positive regulation of lymphocyte differentiation	8.98E-05
GO:0016074	snoRNA metabolic process	9.86E-05

<b>GO term</b>	<b>Neuron Phosphoproteomics: Biological Processes</b>	<b>P-value</b>
GO:0007010	cytoskeleton organization	3.52E-07
GO:0071840	cellular component organization or biogenesis	2.13E-06
GO:0016043	cellular component organization	2.59E-06
GO:0006397	mRNA processing	4.87E-06
GO:0016071	mRNA metabolic process	7.23E-06
GO:0050684	regulation of mRNA processing	6.40E-05
GO:0008380	RNA splicing	7.29E-05
GO:0009987	cellular process	7.29E-05
GO:1903311	regulation of mRNA metabolic process	1.03E-04
GO:1901879	regulation of protein depolymerization	1.18E-04
GO:0006396	RNA processing	1.60E-04

<b>KEGG pathway: up-regulated neuronal proteins</b>	<b>p-value</b>
Spliceosome	1.56E-25
Amyotrophic lateral sclerosis	1.48E-14
Nucleocytoplasmic transport	2.39E-14
Endocytosis	1.87E-13
Huntington disease	5.11E-13
Salmonella infection	9.37E-13
Parkinson disease	9.78E-13
Alzheimer disease	6.35E-11
Prion disease	8.90E-11
Pathways of neurodegeneration - multiple diseases	9.66E-11

<b>KEGG pathway: up-regulated neuronal phosphoproteins</b>	<b>p-value</b>
ErbB signaling pathway	3.18E-08
Axon guidance	5.53E-08
Neurotrophin signaling pathway	2.06E-06
Regulation of actin cytoskeleton	2.33E-06
Pathogenic Escherichia coli infection	6.54E-05
Insulin signaling pathway	8.58E-05
Spliceosome	4.57E-04
Focal adhesion	4.57E-04
Autophagy	5.31E-04
Adherens junction	6.21E-04

<b>KEGG pathway: down-regulated neuronal proteins</b>	<b>p-value</b>
Metabolic pathways	1.69E-13
Ribosome	3.29E-13
Amyotrophic lateral sclerosis	2.01E-09
Parkinson disease	1.36E-08
Pathways of neurodegeneration - multiple diseases	4.91E-08
Thermogenesis	1.33E-07
Huntington disease	1.96E-07
Oxidative phosphorylation	4.27E-07
Valine, leucine and isoleucine degradation	6.49E-07
Endocytosis	6.74E-07

<b>KEGG pathway: down-regulated neuronal phosphoproteins</b>	<b>p-value</b>
Axon guidance	1.40E-07
Insulin signaling pathway	1.49E-05
ErbB signaling pathway	3.74E-05
Regulation of actin cytoskeleton	3.94E-05
Spliceosome	1.76E-04
Endocytosis	6.98E-04
Bacterial invasion of epithelial cells	1.72E-03
Inositol phosphate metabolism	2.19E-03
Focal adhesion	2.19E-03
Phosphatidylinositol signaling system	1.09E-02

Gene	Up-regulated Proteins PPM1D+/tr neurons	Score
CUL4B	Cullin-4B	23.32
SMARCE1	SWI/SNF-related matrix-associated actin-dependent chromatin regulator	17.5
SLK	STE20-like serine/threonine-protein kinase	15.6
POFUT1	GDP-fucose protein O-fucosyltransferase 1	14.79
AUP1	Lipid droplet-regulating VLDL assembly factor AUP1	14.62
DKC1	H/ACA ribonucleoprotein complex subunit	13.41
NEUROG2	Neurogenin-2	12.34
C5orf22	UPF0489	11.57
SVIL	Supervillin	11.33
PJA2	E3 ubiquitin-protein ligase	11.26
TTC28	Tetratricopeptide repeat protein 28	10.5
POLR2C	DNA-directed RNA polymerase II subunit	10.23
PARN	Poly(A)-specific ribonuclease	10.22
NUBP1	Cytosolic Fe-S cluster assembly factor	10.11
EXOSC6	Exosome complex component MTR3	9.89

Gene	Up-regulated phosphoproteins PPM1D+/tr neurons	Score
SRRM1	Serine/arginine repetitive matrix protein 1	34.88
NUCKS1	Nuclear ubiquitous casein and cyclin-dependent kinase substrate 1	33.54
NUCKS1	Nuclear ubiquitous casein and cyclin-dependent kinase substrate 1	32.75
MICAL3	[F-actin]-monooxygenase MICAL3	32.61
NUCKS1	Nuclear ubiquitous casein and cyclin-dependent kinase substrate 1	31.45
CWC22	ubiquitin carboxyl-terminal hydrolase 8	30.88
DCX	Neuronal migration protein doublecortin	30.56
MAP2	Microtubule-associated protein 2	27.14
SCG2	Secretogranin-2	27.12
RAP1GAP2	Rap1 GTPase-activating protein 2	27.10
DCX	Neuronal migration protein doublecortin	26.11
AMER2	APC membrane recruitment protein 2	22.99
CPNE1	Copine-1	22.59
ADCY5	Adenylate cyclase type 5	22.08
TRAPPC14	Trafficking protein particle complex subunit 14	21.89

Gene	Down-regulated Proteins PPM1D+/tr neurons	Score
PELI2	E3 ubiquitin-protein ligase pellino homolog 2	-9.9
EARS2	Probable glutamate--tRNA ligase, mitochondrial	-9.97
NUDT10	Diphosphoinositol polyphosphate phosphohydrolase 3-alpha	-10.02
C3orf49	Putative uncharacterized protein C3orf49	-10.07
IBA57	Putative transferase CAF17, mitochondrial	-10.12
SLC30A1	Zinc transporter 1	-10.17
LACTB	Serine beta-lactamase-like protein LACTB, mitochondrial	-10.72
KRT1	Keratin, type II cytoskeletal 1	-10.88
RAB34	Ras-related protein Rab-34	-11.09
STX4	Syntaxin-4	-11.53
UAP1	UDP-N-acetylhexosamine pyrophosphorylase	-11.61
UPF2	Regulator of nonsense transcripts 2	-13.21
NCAM2	Neural cell adhesion molecule 2	-14.11
TUB	Tubby protein homolog	-16.38
GSTZ1	Maleylacetoacetate isomerase	-21.19

Gene	Down-regulated phosphoprotein PPM1D+/tr neurons	Score
UBR4	E3 ubiquitin-protein ligase	-30.52
RIF1	Telomere-associated protein RIF	-30.80
CANX	Calnexin	-30.84
NEB	Nebulin	-31.28
MADD	MAP kinase-activating death domain protein	-32.21
PLCL1	Inactive phospholipase C-like protein 1	-32.30
SVIL	Supervillin	-33.49
DBN1	Drebrin	-33.63
ANK2	Ankyrin-2	-33.79
ANK2	Ankyrin-2	-34.29
NAA10	N-alpha-acetyltransferase 10	-39.50
ARHGAP35	Rho GTPase-activating protein 35	-45.24
PRKAR2B	cAMP-dependent protein kinase II-beta regulatory subunit	-46.80
SRSF7	Serine/arginine-rich splicing factor 7	-59.87
SRRM1	Serine/arginine repetitive matrix protein 1	-68.44

GO term	Microglia Proteomics: Biological Processes	P-value
GO:0035909	aorta morphogenesis	4.74E-05
GO:0072554	blood vessel lumenization	5.37E-05
GO:0048514	blood vessel morphogenesis	8.88E-05
GO:0061314	Notch signaling involved in heart development	1.52E-04
GO:0035912	dorsal aorta morphogenesis	1.52E-04
GO:0009311	oligosaccharide metabolic process	1.59E-04
GO:0044242	cellular lipid catabolic process	2.40E-04
GO:0010885	regulation of cholesterol storage	3.11E-04
GO:0032621	Interleukin 18 production	3.51E-04
GO:0021983	pituitary gland development	4.44E-04
GO:0090136	epithelial cell cell adhesion	4.96E-04
GO:0048844	artery morphogenesis	5.95E-04
GO:1900227	positive regulation of NLRP3 inflammasome complex assembly	5.98E-04

GO term	Microglia Phosphoproteomics: Biological Processes	P-value
GO:0008380	RNA splicing	2.24E-20
GO:0000398	mRNA splicing, via spliceosome	2.80E-19
GO:0051056	regulation of small GTPase mediated signal transduction	5.03E-18
GO:0006397	mRNA processing	1.32E-17
GO:0035556	intracellular signal transduction	1.49E-17
GO:0006338	chromatin remodeling	3.04E-13
GO:0006325	chromatin organization	2.07E-12
GO:0006468	protein phosphorylation	3.39E-11
GO:0007010	cytoskeleton organization	1.19E-10
GO:0006974	cellular response to DNA damage stimulus	2.12E-10

<b>KEGG pathway up-regulated proteins microglia</b>	<b>p-value</b>	<b>KEGG pathway down-regulated proteins microglia</b>	<b>p-value</b>
Lysosome	6.94E-07	Amyotrophic lateral sclerosis	1.16E-08
Parkinson disease	4.53E-06	Huntington disease	8.41E-07
Prion disease	1.77E-05	Phagosome	1.35E-06
RNA transport	6.67E-05	Salmonella infection	1.71E-05
Citrate cycle (TCA cycle)	8.17E-05	Prion disease	6.06E-05
Alzheimer disease	1.52E-04	Pathways of neurodegeneration	6.77E-05
Cholesterol metabolism	2.22E-04	Proteasome	1.33E-04
Aminoacyl-tRNA biosynthesis	2.23E-04	Pathogenic Escherichia coli infection	1.33E-04
Glycolysis / Gluconeogenesis	2.48E-04	Vibrio cholerae infection	2.28E-04
Phagosome	4.26E-04	RNA transport	2.49E-04

<b>KEGG pathway up-regulated phosphoproteins microglia</b>	<b>p-value</b>	<b>KEGG pathway down-regulated phosphoproteins microglia</b>	<b>p-value</b>
Spliceosome	1.47E-07	Spliceosome	5.28E-08
Yersinia infection	3.92E-05	Viral life cycle - HIV-1	7.29E-07
Rap1 signaling pathway	7.68E-05	Regulation of actin cytoskeleton	8.36E-07
Shigellosis	1.60E-04	Thyroid hormone signaling pathway	1.97E-06
Insulin signaling pathway	7.70E-03	Platelet activation	1.05E-05
NOD-like receptor signaling pathway	1.79E-02	Fc gamma R-mediated phagocytosis	2.77E-05
Transcriptional misregulation in cancer	2.41E-02	Endocytosis	4.57E-05
Adherens junction	3.31E-02	Renal cell carcinoma	5.48E-05
Fc gamma R-mediated phagocytosis	3.56E-02	ErbB signaling pathway	5.51E-05
Platelet activation	3.71E-02	Insulin signaling pathway	5.53E-05

Gene	Up-regulated proteins PPM1D+/tr microglia	Score	Gene	Down-regulated proteins PPM1D+/tr microglia	Score
CDC34	Ubiquitin-conjugating enzyme E2	29.63	ACOD1	Cis-aconitate decarboxylase	-14.10
GBP5	Guanylate-binding protein 5	28.63	DDX54	ATP-dependent RNA helicase	-14.14
CD2BP2	CD2 antigen cytoplasmic tail-binding protein 2	26.46	HERC5	E3 ISG15--protein ligase	-14.51
KLHDC4	Kelch domain-containing protein 4	26.33	VPS33A	Vacuolar protein sorting-associated protein 33A	-15.50
SOX3	Transcription factor SOX-3	22.47	SLC38A2	Sodium-coupled neutral amino acid transporter 2	-16.01
PELI1	E3 ubiquitin-protein ligase pellino homolog 1	21.52	MMP13	Collagenase 3	-16.11
MAN1B1	Endoplasmic reticulum mannosyl-oligosaccharide 1,2-alpha-mannosidase	21.44	CDK1	Cyclin-dependent kinase 1	-16.67
MYEF2	Myelin expression factor 2	20.04	GBP1	Guanylate-binding protein 1	-16.68
TEP1	Telomerase protein component 1	18.3	PARP9	Protein mono-ADP-ribosyltransferase PARP9	-16.91
CCNK	Cyclin-K	17.87	LIMD2	LIM domain-containing protein 2	-20.34
DLL4	Delta-like protein 4	17.7	POGZ	Pogo transposable element with ZNF domain	-28.22
AZI2	5-azacytidine-induced protein 2	17.28	SLC38A10	Putative sodium-coupled neutral amino acid transporter 10	-30.52
GSTM1	Glutathione S-transferase Mu 1	16.66	HERC6	Probable E3 ubiquitin-protein ligase HERC6	-31.45
DHRX	Dehydrogenase/reductase SDR family member on chromosome X	16.03	APOBEC3G	DNA dC->dU-editing enzyme APOBEC-3G	-33.14
ANGEL2	Protein angel homolog 2	14.85	TANK	TRAF family member-associated NF-kappa-B activator	-46.18

Gene	Up-regulated phosphoproteins PPM1D+/tr microglia	Score	Gene	Down-regulated phosphoproteins PPM1D+/tr microglia	Score
PXN	Paxillin	14.95	CLASP2	CLIP-associating protein 2	-20.3
DDX54	ATP-dependent RNA helicase DDX54	8.97	RETREG2	Reticulophagy regulator 2	-20.53
TOP2B	DNA topoisomerase 2-beta	8.85	MAP4K4	Mitogen-activated protein kinase kinase kinase 4	-20.92
MACF1	Microtubule-actin cross-linking factor 1	8.21	TBC1D2BTBC1	TBC1 domain family member 2B	-21.38
SRRM1	Serine/arginine repetitive matrix protein 1	8.04	RASAL3	RAS protein activator like-3	-21.7
ATP6V0A2	V-type proton ATPase 116 kDa subunit a2	7.9	AMPD3	AMP deaminase 3	-21.94
PARN	Poly(A)-specific ribonuclease PARN	7.73	CD2BP2	CD2 antigen cytoplasmic tail-binding protein 2	-22.21
CCNY	Cyclin-Y	7.72	SNTB1	Beta-1-syntrophin	-25.43
TRAFD1	TRAF-type zinc finger domain-containing protein 1	7.29	PI4KB	Phosphatidylinositol 4-kinase beta	-26
TRAFD1	TRAF-type zinc finger domain-containing protein 1	7.08	SUDS3	Sin3 histone deacetylase corepressor complex component SDS3	-26.29
TMEM230	Transmembrane protein 230	6.7	VPS50	Syndetin	-29.52
SRRM1	Serine/arginine repetitive matrix protein 1	6.65	SNX5	Sorting nexin-5	-30.13
STX11	Syntaxin-11	6.36	UFL1	E3 UFM1-protein ligase 1	-39.21
ARHGEF2	Rho guanine nucleotide exchange factor 2	6.3	FLII	Protein flightless-1 homolog	-41.86
DKC1	H/ACA ribonucleoprotein complex subunit DKC1	6.01	SERF2	Small EDRK-rich factor 2	-62.15

<b>GO term</b>	<b>LPS Microglia Proteomics: Biological Processes</b>	<b>P-value</b>
GO:0032715	negative regulation of interleukin-6 production	3.23E-05
GO:0072310	glomerular epithelial cell development	3.44E-05
GO:0072015	glomerular visceral epithelial cell development	3.44E-05
GO:0034446	substrate adhesion-dependent cell spreading	1.08E-04
GO:0015850	organic hydroxy compound transport	1.39E-04
GO:0031589	cell-substrate adhesion	1.63E-04
GO:0072359	circulatory system development	1.90E-04
GO:2000351	regulation of endothelial cell apoptotic process	2.08E-04
GO:0003014	renal system process	2.51E-04
GO:0006003	fructose 2,6-bisphosphate metabolic process	3.31E-04

<b>GO term</b>	<b>LPS Microglia Phosphoproteomics: Biological Processes</b>	<b>P-value</b>
GO:0008380	RNA splicing	2.32E-20
GO:0000398	mRNA splicing, via spliceosome	2.89E-19
GO:0051056	regulation of small GTPase mediated signal transduction	5.17E-18
GO:0006397	mRNA processing	1.37E-17
<b>GO:0035556</b>	<b>intracellular signal transduction</b>	1.56E-17
<b>GO:0006338</b>	<b>chromatin remodeling</b>	3.11E-13
<b>GO:0006325</b>	<b>chromatin organization</b>	2.14E-12
<b>GO:0006468</b>	<b>protein phosphorylation</b>	3.52E-11
<b>GO:0007010</b>	<b>cytoskeleton organization</b>	1.22E-10
<b>GO:0006974</b>	<b>cellular response to DNA damage stimulus</b>	2.18E-10
<b>GO:0045944</b>	<b>positive regulation of transcription from RNA polymerase II promoter</b>	2.86E-10
<b>GO:0051301</b>	<b>cell division</b>	4.59E-09
<b>GO:0030036</b>	<b>actin cytoskeleton organization</b>	9.04E-09
<b>GO:0007165</b>	<b>signal transduction</b>	1.01E-08
<b>GO:0090630</b>	<b>activation of GTPase activity</b>	2.75E-08

<b>KEGG pathway up-regulated proteins LPS microglia</b>	<b>p-value</b>	<b>KEGG pathway down-regulated proteins LPS microglia</b>	<b>p-value</b>
Lysosome	2.38E-22	Spliceosome	6.00E-15
Metabolic pathways	1.22E-13	Nucleocytoplasmic transport	2.12E-13
Huntington disease	6.41E-12	Amyotrophic lateral sclerosis	1.68E-12
Parkinson disease	1.14E-11	Salmonella infection	1.86E-12
Prion disease	5.47E-11	Ribosome	1.15E-10
Amyotrophic lateral sclerosis	5.06E-10	Protein processing in endoplasmic reticulum	2.03E-10
Oxidative phosphorylation	1.25E-09	Epstein-Barr virus infection	2.74E-10
Chemical carcinogenesis - reactive oxygen species	4.44E-08	Carbon metabolism	1.08E-09
Pathways of neurodegeneration - multiple diseases	5.90E-08	Shigellosis	1.67E-09
Neutrophil extracellular trap formation	6.17E-08	Leishmaniasis	2.50E-08
Proteasome	1.43E-07	Metabolic pathways	2.64E-08
		Coronavirus disease - COVID-19	3.92E-08
		Influenza A	7.27E-08

<b>KEGG pathway up-regulated phosphoproteins LPS microglia</b>	<b>p-value</b>	<b>KEGG pathway down-regulated phosphoproteins LPS microglia</b>	<b>p-value</b>
Rap1 signaling pathway	6.29E-06	Spliceosome	2.07E-09
Yersinia infection	7.87E-06	Regulation of actin cytoskeleton	7.01E-07
Platelet activation	8.81E-06	Viral life cycle - HIV-1	7.27E-05
Regulation of actin cytoskeleton	7.58E-05	Thyroid hormone signaling pathway	9.62E-05
Fc gamma R-mediated phagocytosis	1.78E-04	ErbB signaling pathway	1.37E-04
Adherens junction	2.10E-04	Shigellosis	1.59E-04
Shigellosis	2.24E-04	Insulin signaling pathway	1.78E-04
Pathogenic Escherichia coli infection	2.59E-04	Rap1 signaling pathway	3.22E-04
Thyroid hormone signaling pathway	4.00E-04	Leukocyte transendothelial migration	4.17E-04
Chemokine signaling pathway	5.52E-04	Yersinia infection	5.00E-04

Gene	Up-regulated proteins PPM1D+/tr LPS microglia	Score
UHRF1BP1	UHRF1-binding protein 1	60.28
GBA1	Lysosomal acid glucosylceramidase	55.35
ETNK1	Ethanolamine kinase 1	37.18
PYGL	Glycogen phosphorylase, liver form	34.4
UGP2	UTP--glucose-1-phosphate uridylyltransferase	32.4
RAB11A	Ras-related protein Rab-11A	30.74
CSK	Tyrosine-protein kinase CSK	29.54
SLC25A35	Solute carrier family 25 member 35	27.87
PAFAH2	Platelet-activating factor acetylhydrolase 2, cytoplasmic	27.23
FGG	Fibrinogen gamma chain	26.9
LAMB2	Laminin subunit beta-2	25.49
ZBTB33	Transcriptional regulator Kaiso	24.49
LYPLA2	Acyl-protein thioesterase 2	22.79
STARD3	StAR-related lipid transfer protein 3	22.75
SIAE	Sialate O-acetyltransferase	22.49

Gene	Up-reg. phosphoproteins PPM1D+/tr LPS microglia	Score
UBR4	E3 ubiquitin-protein ligase	62.42
UBR4	E3 ubiquitin-protein ligase	47.723
IL16	Pro-interleukin-16	38.099
LBR	Delta(14)-sterol reductase	32.377
TBC1D10B	TBC1 domain family member 10B	30.032
UBR4	E3 ubiquitin-protein ligase	29.951
UBR4	E3 ubiquitin-protein ligase UBR4	28.137
PI4KA	Phosphatidylinositol 4-kinase alpha	26.685
LTB4R	Leukotriene B4 receptor 1	23.842
PLXNC1	Plexin-C1	21.067
SMARCA2	Probable global transcription activator SNF2L2	20.538
RBM33	RNA-binding protein 33	19.82
SIPA1L1	Signal-induced proliferation-associated 1-like protein 1	17.973
PLXNC1	Plexin-C1	17.862
HNRNPU	Heterogeneous nuclear ribonucleoprotein U	17.634

Gene	Down-regulated proteins PPM1D+/tr LPS microglia	Score
PI4KA	Phosphatidylinositol 4-kinase alpha	-29.3389
RPL18	60S ribosomal protein L18	-29.6675
DDX59	Probable ATP-dependent RNA helicase DDX59	-31.5494
SPRYD7	SPRY domain-containing protein 7	-32.4876
EPS8	Epidermal growth factor receptor kinase substrate 8	-33.9319
CBR3	Carbonyl reductase [NADPH]	-34.3485
HSPBAP1	HSPB1-associated protein 1	-37.1573
MTA1	Metastasis-associated protein MTA1	-37.6405
CPM	Carboxypeptidase M	-39.6778
KCTD5	BTB/POZ domain-containing protein KCTD5	-42.0408
NUBP2	Cytosolic Fe-S cluster assembly factor NUBP2	-42.8254
TAX1BP3	Tax1-binding protein 3	-43.4695
HSPB11	Intraflagellar transport protein 25 homolog	-47.3325
HAS1	Hyaluronan synthase 1 OS=Homo sapiens	-50.9275
UBR4	E3 ubiquitin-protein ligase UBR4	-65.0923

Gene	Down-reg. phosphoproteins PPM1D+/tr LPS microglia	Score
IRAG2	Inositol 1,4,5-triphosphate receptor associated 2	-37.17
HSP90AB1	Heat shock protein HSP 90-beta	-39.11
KIAA0930	Uncharacterized protein KIAA0930	-39.54
BCLAF1	Bcl-2-associated transcription factor 1	-43.15
IRF2BP1	Interferon regulatory factor 2-binding protein 1	-45.51
RPL23A	60S ribosomal protein L23a	-46.79
PFKFB3	6-phosphofructo-2-kinase/fructose-2,6-bisphosphatase 3	-48.40
PRRC2C	Protein PRRC2C	-52.17
PRPF4B	Serine/threonine-protein kinase PRP4 homolog	-53.02
DVL3	Segment polarity protein dishevelled homolog DVL-3	-53.07
FNBP1	Formin-binding protein 1	-58.01
LARP7	La-related protein 7	-58.89
RBM25	RNA-binding protein 25	-63.53
HNRNPA1	Heterogeneous nuclear ribonucleoprotein A1	-64.67
RASAL3	RAS protein activator like-3	-65.28